DEVELOPMENT OF AN ANISOTROPIC COPPER CAPILLARY ALGINATE SCAFFOLD WITH ORIENTED TUBE LIKE PORES FOR PHEOCHROMACYTOMA-12 CELL GUIDANCE

A DISSERTATION SUBMITTED

BY

ANITHA ISAIAH

IN PARTIAL FULFILLMENT OF THE REQUIREMENTS

FOR THE DEGREE OF

MASTER OF PHILOSOPHY

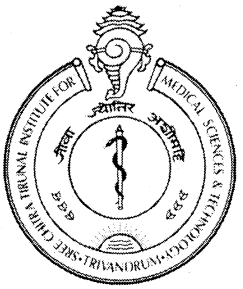

SREE CHITRA TIRUNAL INSTITUTE FOR MEDICAL SCIENCES AND TECHNOLOGY
TRIVANDRUM – 695 011

DECLARATION

I, **Anitha Isaiah**, hereby declare that I had personally carried out the work depicted in the dissertation entitled "**Development of an anisotropic copper capillary alginate scaffold with oriented tube like pores for Pheochromacytoma-12 cell guidance**" under the direct supervision of of **Dr. Anoopkumar Thekkuveettil, Scientist F, Division of Molecular Medicine,** Biomedical Technology Wing, Sree Chitra Tirunal Institute for Medical Sciences and Technology, Thiruvananthapuram, Kerala, India. External help sought are acknowledged.

Signature

Anitha Isaiah

SREE CHITRA TIRUNAL INSTITUTE FOR MEDICAL SCIENCES & TECHNOLOGY
TRIVANDRUM – 695011, INDIA
(*An Institute of National Importance under Govt. of India with the status of University by an Act of Parliament in 1980*)

CERTIFICATE

This is to certify that the dissertation entitled "**Development of an anisotropic copper capillary alginate scaffold with oriented tube like pores for Pheochromacytoma-12 cell guidance"** submitted by **Anitha Isaiah** in partial fulfilment for the Degree of Master of Philosophy in Biomedical Technology to be awarded by this Institute. The entire work was done by **him/her** under my supervision and guidance at Division **of Molecular Medicine**, Biomedical Technology Wing, Sree Chitra Tirunal Institute for Medical Sciences and Technology (SCTIMST), Thiruvananthapuram-695012

Thiruvananthapuram
Date 31/07/2011

Signature
Dr. Anoopkumar Thekkuveettil

The Dissertation

Entitled

DEVELOPMENT OF AN ANISOTROPIC COPPER CAPILLARY ALGINATE SCAFFOLD WITH ORIENTED TUBE LIKE PORES FOR PHEOCHROMACYTOMA-12 CELL GUIDANCE

Submitted

By

Anitha Isaiah

For

Master of Philosophy

of

SREE CHITRA TIRUNAL INSTITUTE FOR MEDICAL SCIENCES AND TECHNOLOGY

TRIVANDRUM – 695 011

Evaluated and approved

by

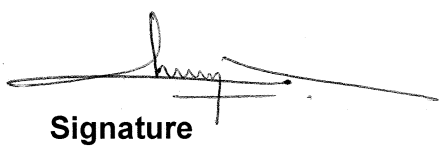

Signature

Name of Supervisor

Signature

Examiner's name and Designation

Dr. Rekha M. R
Scientist - C

Acknowledgements

First and foremost I express my sincere gratitude to **Dr. Anoopkumar Thekkuveettil**, my guide and mentor for his excellent guidance and support during the entire course of this work.

I am grateful to **The Director,** SCTIMST, **The Head,** BMT Wing and **The Deputy Registrar,** SCTIMST and **The Division of Academic Affairs**, BMT Wing for providing the necessary facilities for the successful completion of my course.

I would also like to thank **Dr. Lissy K Krishnan, Dr. Kalyankrishnan V, and Dr. Roy Joseph** for their valuable suggestions which helped me overcome certain stumble blocks I faced during the project.

I thank **Mr. Jose Jacob** for his help and support in times of need.

Coffee and words of wisdom, for which I would like to thank my colleagues, **Anupriya, Bejoy, Moidu, Sarish, Sooraj, Suryashree and Swapna**, at the Division of Molecular Medicine for their support and help when the days were glum. They have taught me quite a few things both about science and life.

I would also like to acknowledge the help and support of **Shaiju, Leksmi, Durga Das and Kiran**.

I express my sincere thanks to my batchmates, **Aneesh, Ajoy, Dinesh, Binnu, Revathy, Karthick** and **Lekshmi** for their help and constructive criticism.

Without their unconditional love and infinite patience of my **parents** from my childhood to this day, I would never have made it this far or through any of the tough times.

Finally, I humbly acknowledge the blessing showered upon me by the **Lord almighty**, without His blessings nothing is possible. The Lord is my refuge and strength, a tested help in times of trouble and worries.

Abbreviations

°C	Degree Celsius
µl	Microliter
µm	Micromolar
BSA	Bovine Serum Albumin
CCAG	Copper Capillary Alginate Gel
CNS	Central Nervous System
DMEM	Dulbecco's Modified Eagle Medium
DMEM:F12	Dulbecco's Modified Eagle Medium/Nutrient Mixture F-12 Ham
DNA	Deoxy ribo Nucleic Acid
ECM	Extracellular Matrix
EDS	Energy Dispersive Spectrometry
g	Gram
HDI	Hexamethylene Diisocyanate
HEK	Human Embryonic Kidney
IU	International Unit
LCST	Lower Critical Solution Temperature
min	Minute
mL	Milliliter
ng	Nanogram

NGF	Nerve Growth Factor
PBS	Phosphate Buffered Saline
PC 12	Pheochromacytoma 12
PEO	Poly Ethylene Oxide
PLA	Poly Lactic Acid
PNS	Peripheral Nervous System
PVA	Poly Vinyl Alcohol
RCCAG	Raw Copper Capillary Alginate Gel
SEM	Scanning Electron Microscopy
UV	Ultraviolet

Table of Contents

List of Figures

Synopsis

This work demonstrates that alginate based capillary hydrogels represent a unique group of biopolymer scaffolds, which creates an environment that could facilitate neuronal regeneration and neurite extension. The idea was that the highly oriented channels formed within the scaffold could promote regeneration and perhaps shed some light on the mechanism of axonal pathfinding. The ability to vary the capillary diameters of the scaffold is an added advantage which could help in regulating number of axons growing within a capillary. When compared to the other methods like etching and micropatterning this method is easier and less expensive. In this study, the scaffold was successfully synthesized and stabilized by cross linking with hexamethylene diisocyanate. By varying the concentration of alginate used in the scaffold, the capillary diameters could be varied. Different capillary dimensions were obtained by varying the concentration of copper ions for the ionotropic gel formation. Most of the microchannels fabricated by various researchers vary in range between 0.5μm to 120μm (Flynn *et al.* 2003; Stokols and Tuszynski 2006). The choice of copper nitrate solution as the electrolyte was based on the data presented by Theile, who actually summarized an ionotropic series. According to this series Cu^{2+} ions created capillaries in alginate ranging between 8-35μm (Thiele 1947) which is not in direct correlation with the data obtained (12.1-92.3 μm) in this study. This difference maybe because of the differences in the starting material and thickness of the gel body studied. There are many methods for the creation of guidance channels like longitudinal capillaries, micro and nanofibres or microsized grooves within scaffolds. Chemical cues such as matrix proteins, neurotrophic factors could also help in neuronal guidance and regeneration (Bellamkonda *et al.* 1995; Schmidt and Leach 2003). The copper capillary alginate scaffold degraded away when placed in water or PBS by exchanging free ions with the ions in the solution. The stabilization of the scaffold was done by cross linking with HDI (Prang *et al.* 2006) and this decreased the degradation of the Copper capillary alginate gel scaffold and hence can be utilized for *in vitro* work. Furthermore, the scaffold was coated with chitosan to enhance cell attachment. Previous

studies suggest that chitosan enhances neuronal attachment (Cao *et al.* 2009). Our study shows, cross linking and coating the scaffold with chitosan did not alter the capillary structure or dimensions. The copper ions leaching out from the scaffold could prove to be toxic to the cells, therefore it was washed successively with hydrochloric acid to exchange the copper ions with protons. Energy dispersive spectroscopy analysis showed peaks for chlorine due to successive Hydrochloric acid washes, but EDS failed to show peaks for copper. Micro CT analysis helped to elucidate the pore structure of the scaffold and also helped to understand that concentration of alginate played a role in the capillary dimensions. It also revealed that the CCAG scaffold fabricated with 1% alginate solution, majority of the capillaries fall below 64μm with a highest pore size of 112μm and in the scaffold with 2% alginate there is a significant shift towards higher size capillaries above 32μm to a maximum size of 144μm. The biocompatibility of the scaffold and cellular attachment were studied using Pheochromacytoma 12 cells and HEK cells. The results suggest that extensive cross linking does induce cell toxicity (25%) and affects the cellular attachment to a greater extend. Future work is still needed to assess the full potential of this unique type of scaffolds.

Introduction

Chapter 1

Introduction

1.1 Background

Regeneration strategies for the Peripheral and Central Nervous system has only met with limited amount of success due to the complicated nature of the neuronal cells and the lack of information pertaining to injury and repair in the nervous system (An *et al.* 2006). The response to injury by the Central Nervous System (CNS) and Peripheral Nervous System (PNS) is markedly different. Following injury in the CNS, the non permissive environment prevailing within the CNS does not encourage the regeneration of injured axons. Several glycoproteins in the native extracellular environment of the CNS are inhibitory to regeneration. In the PNS, the myelin debris and glial scars are removed by macrophages and the Schwann cells help in regrowth. When compared to the rate of macrophage infiltration in the PNS, the infiltration rate is much slower in the CNS delaying the removal of inhibitory myelin. The formation of glial scar, oligodendrocytes and myelin debris is responsible for the creation of a non permissible environment for the regeneration of axons (Schmidt and Leach 2003). Many strategies have been applied, such as cell therapy, neural tissue engineering, exogenous delivery of growth factors for improving the regeneration potential of neurons with variable amount of success. Autografts have been reported to facilitate neuroregeneration over considerable distances but they have their own disadvantages such as lack of donor supply to the graft site and the need for secondary surgical sites. The functional outcomes of this procedure is not very encouraging (Meek and Coert 2002). In the case of CNS damage, repair strategies should not only focus on neuronal survival and axonal growth but also in establishing functional synaptic connections with adjacent neurons.

Tissue engineering has been defined as an interdisciplinary field that applies the principles of engineering and life sciences towards the development of biological substitutes that restore, maintain or improve the tissue function. This field also focuses on the development of three dimensional support matrices called scaffolds to act like a template and thereby assist in the growth and regeneration of tissues. The development of such scaffolds plays a crucial role in repair, restoration and regeneration strategies (Langer and Vacanti 1993). Crucial to the choice of regeneration strategy is the choice of material, whether it is biodegradable or bioinert. Biodegradable polymers have been used as a method for the delivery of growth factors and therefore could be used for the controlled growth delivery of growth factors to the CNS (Cascone *et al.* 1995; Chen and Mooney 2003; Burdick *et al.* 2006). They could be used in the repair of damaged neurons in the central and peripheral nervous system. Biodegradable polymers of natural origin promise to be interesting candidates for being chosen as scaffolds to promote neuronal regeneration. Biopolymers because of their natural origin allow one to design and engineer biomaterial systems that function at the molecular level, and often minimize chronic inflammation. Also, to an extent their properties resemble the tissue that they replace. They are often soluble in water, allowing mild fabrication conditions that are relatively harmless to the bioactivity of the growth factors (Lee *et al.* 2011). Natural biomaterials also promote neuronal and glial cell adhesion (Straley *et al.* 2010). Hence natural biopolymers are much more suitable for implantation than their synthetic counterparts. Hydrogels can be easily molded into various shapes or directly injected at the site of injury. They can function as scaffolds through which the nerves can regenerate. A scaffold for nerve regeneration should be able to deliver neurotrophic growth factors or cells and desirably have channels in them which will mimic the natural fascicular architecture (Schmidt and Leach 2003). It is believed that scaffolds with channels and fibres promote regeneration chiefly by increasing the the surface area to which the cells and regenerating axons can attach (Straley *et al.* 2010). The advantages of having microchannels on neurite guidance has inspired the fabrication of hydrogel scaffolds with uniaxial pores and channels (Stokols and Tuszynski 2006). Anisotropic capillary

hydrogels created by ionotropic gelation of alginate have been studied for various tissue engineering strategies. These capillary hydrogels have been shown to form via a self-organizing process that is driven by the unidirectional diffusion of divalent cations through sodium alginate sols. And studies have shown that they promote the longitudinally oriented elongation of axons in the CNS (Pawar *et al.* 2011).

Pheochromacytoma-12 (PC 12) cell line, derived from the rat adrenal medulla can differentiate into terminal neurons in the presence of Nerve Growth Factor (Greene and Tischler 1976). Rat pheochromacytoma-12 cell line has been used as a neuronal model cell line (Banker and Goslin 1998). Some features of the cell line including production of neurites and appearance of electrical excitability in response to Nerve Growth Factor (NGF) makes it a candidate for being considered as a model cell line for neurobiological investigations (Zhou *et al.* 2006).

This study focuses on the development of an anisotropic copper capillary alginate scaffold with oriented tube like pores for rat pheochromacytoma-12 cell guidance for studying its neurite growth and guidance.

1.2 Review of Literature

1.2.1 Introduction

The nervous system is chiefly made up of neurons and glial cells .Of which the neurons form the functional unit of the nervous system. Neurons are highly specialized, excitable post mitotic cells. It consists of three parts (1) the cell body or soma (2) the dendrites and (3) the axon.

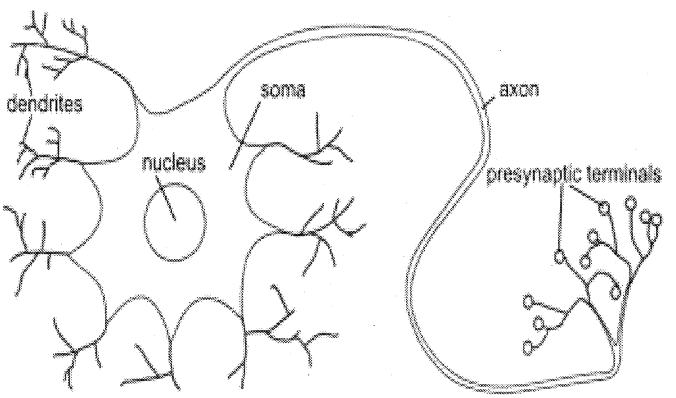

Figure 1: Typical structure of a neuron. Adapted from Franz and Guck, 2010

A typical neuron consists of three parts, the cell body, the dendrites and the axon

In order to form a functional neuronal network, the neurons need to interconnect by forming synapses between the dendrites and axons. Dendrites are involved in receiving signals and they are highly branched and connect to as many axons in the near vicinity of the cell. Unlike the axon, they cannot extend for a longer distance from the

cell body (Ropper *et al.* 2009) . An axon is the longest branch emanating from the cell body and is specialized for sending information.

1.2.2 Neuronal growth

Control over neuronal growth is a fundamental objective in neuroscience, cell biology, developmental biology, biophysics, and biomedicine. It is particularly important for the formation of neural circuits *in vitro*, as well as nerve regeneration *in vivo* (Ehrlicher *et al.* 2002). Initial development and continued restructuring of dendritic and axonal processes during periods of plasticity or recovery from injury is thought to be dependent, in large part, on activity of their growth cones (Shibata *et al.* 1998). Growth cones of developing and regenerating neurites receive specific navigational instructions through recognition of particular environmental cues (Stirling and Dunlop 1995).

1.2.2.1 Growth Cones

Growth cones are specialized structures seen at the tip of extending neurites. They were first observed in fixed chick embryonic tissues by Ramon y Cajal. A growth cone is comprised of three distinct regions (Rajnicek and McCaig 1997): (1) the central domain which contains the microtubules and organelles (2) the lamellipodium, which is made up of a meshwork of filamentous actin (F-actin) (3) finger like extensions referred to as the filopodia, which is made of bundles of F-actin. The proximal region of the growth cone is packed with mitochondria, endosomes and multi-lamellated membrane bound vesicles. These exhibit amoeboid movement as the growth cone surfs the environment.Neuronal migration, guidance and extension depend on the actin filament cytoskeleton which generate protrusive forces allowing the cell to migrate forward and change shapes by extending the processes. The growth cone is not only the machinery that drives axon extension, but also the converging target of axon growth regulatory signals, including inhibitory signals in the central nervous system (Dent and Gertler 2003).

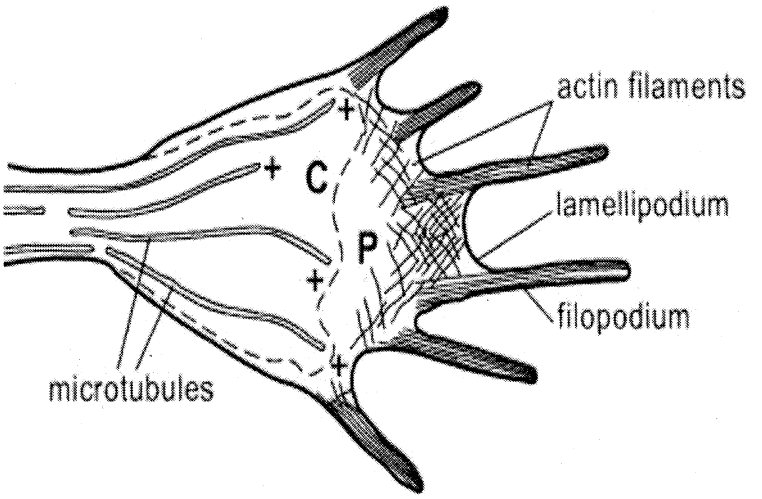

Figure 2. The neuronal growth cone. Two types of cytoskeletal elements predominate in growth cones. Microtubules are found in abundance in the organelle-rich central domain (C), with some extending to the base of filopodia at the leading edge. The faster growing plus ends of microtubules are indicated. In the organelle-poor peripheral domain (P), actin filaments predominate, forming tight bundles in filopodia and a dense interwoven meshwork at the leading edge and in lamellipodia (Mueller 1999).

The filopodia and lamellipodia are two major cellular structures attributed to cell motility. Axon extension typically consists of three steps (Dent and Gertler 2003):

1. Protrusion of filopodia and lamellipodia that generates new intercellular space for the cytoplasm to advance into as the axon moves forward

2. Engorgement, which involves movement of cytoplasm along with microtubules and organelles into the new protruded structures

3. Consolidation, that brings a termination of protrusion from the sides of the growth cones. This basically helps in the maintenance of a polarized migratory structure at the tip of the axon.

Protrusion occurs by the rapid extensions of filopodia and thin lamellar protrusions, often between filopodia. These extensions are primarily composed of bundled and mesh-like F-actin networks. Engorgement occurs when microtubules invade protrusions bringing membranous vesicles and organelles (mitochondria, endoplasmic reticulum). Consolidation occurs when the majority of F-actin depolymerizes in the neck of the growth cone, allowing the membrane to shrink around the bundle of microtubules, forming a cylindrical axon shaft (Dent and Gertler 2003). This process also occurs during the formation of collateral branches off the growth cone or axon shaft.

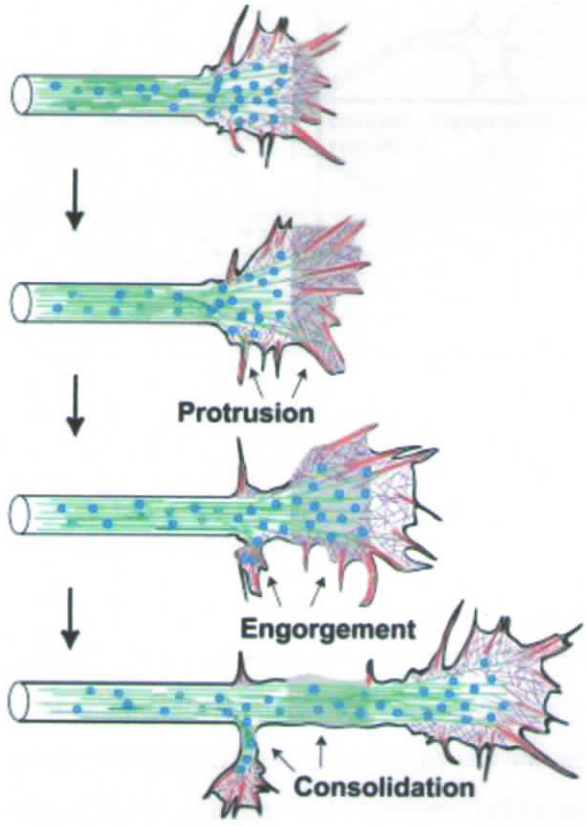

Figure 3: Stages of Axon and Branch Growth. Three stages of axon outgrowth have been termed protrusion, engorgement, and consolidation (Dent and Gertler 2003)

Growth cones have several roles in neurite growth and guidance. They act as locomotory organelles and they are the sites of neurite assembly. The finger-like

protrusions, filopodia, and web-like cytoplasmic veils, called lamellipodia play important roles in detecting molecular cues for growth cone adhesion and motility. The actin cytoskeleton is crucial for determining the shape of growth cone filopodia and lamellipodia (Tanaka and Sabry 1995).

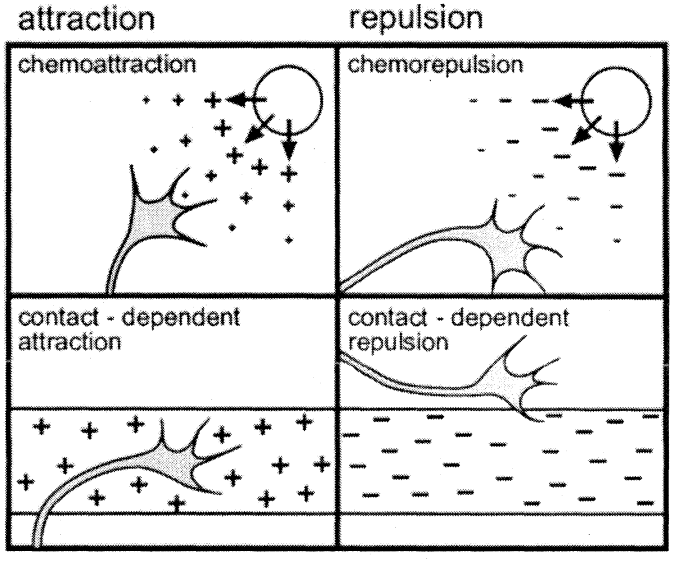

Figure 4: Growth cone guidance mechanisms. Guidance mechanisms are classified as being either attractive or repulsive, with both acting over long- (chemoattraction or chemorepulsion) or shortrange distances (contact-dependent attraction or repulsion). For a growth cone, such a distinction might be irrelevant, assuming that it uses the same receptors for detecting diffusible or stationary guidance cues (Mueller 1999).

Neuronal growth cones navigate over long distances along specific pathways to find their correct targets. Growth cones appear to be guided by at least four different mechanisms: contact attraction, chemoattraction, contact repulsion and chemorepulsion. It has been found that these mechanisms act simultaneously and in a coordinated manner to direct the pathfinding (Tessier-Lavigne and Goodman 1996). In contrast to advancing growth cones, injured axons form retraction bulbs, which contain disorganized microtubules that fail to extend into the periphery.Thus, reorganization of the microtubule network and subsequent formation of an advancing growth cone might promote axon growth and overcome multiple inhibitory signals.(Ertürk *et al.* 2007)

1.2.2.2 Axonal Guidance

Axons are guided along specific pathways by attractive and repulsive cues in the extracellular environment. Genetic and biochemical studies have led to the identification of highly conserved families of guidance molecules, including netrins, Slits, semaphorins and ephrins. Guidance cues steer axons by regulating cytoskeletal dynamics in the growth cone through signaling pathways (Dickson 2002).

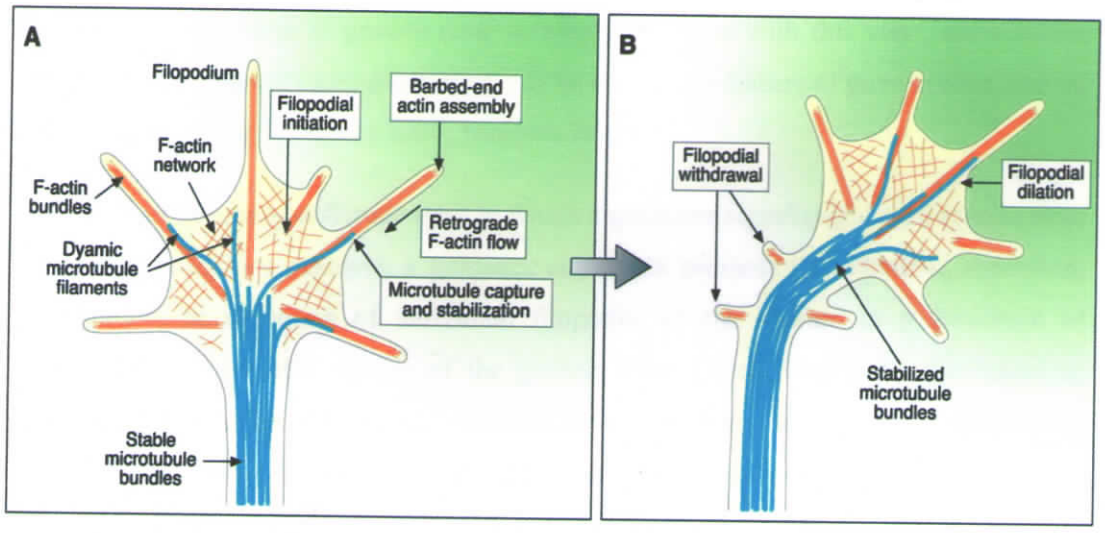

Figure 5. A model showing one way in which a growth cone might turn toward an attractant (Dickson 2002).

Growth cone turning is a complex process in which actin- based motility is utilized to produce directed microtubule advance. Actin filaments are basically divided into two groups: the dense, parallel filaments that radiate outward and into filopodia; and intervening networks of loosely interwoven filaments (Lewis and Bridgman 1992). Filopodial filaments are oriented with their fast growing barbed ends toward the fillopodial tip. The extension and retraction of a filopodium reflect the balance between the actin polymerization at barbed ends and the retrograde flow of entire filaments. Filopodia often extend asymmetrically before the entire growth cone turns, and without

filopodia, growth cones become disoriented. The precise role of filopodia in growth cone turning remains unclear, but they have been postulated to steer the growth cone by differential adhesion, generating mechanical force or transducing distal signals (Davenport *et al.* 1993). These filaments display the classic properties of dynamic instability, extending and retracting as they explore the peripheral region of the growth cone. These dynamic microtubules grow preferentially along the filopodial actin filaments, and the capture or stabilization of microtubule bundles in a specific filopodium may be a critical event in growth cone turning. Consistent with this view, stabilization and dilation of a single filopodium appear to be a common feature of growth cone turning in vivo (Isbister and O'Connor 2000; Dickson 2002).

There are many different ways in which a guidance signal might intervene to steer the growth cone. For example, a guidance cue might promote the initiation, extension, stabilization, or retraction of individual filopodia, or the capture or stabilization of microtubules in specific regions of the growth cone. Likely targets for the signaling pathways downstream of guidance receptors are therefore molecules such as Arp2/3 (to nucleate new actin filaments), Ena/VASP proteins (to promote filament elongation), adhesion molecules (to couple actin filaments to the substrate), and myosins (to regulate the retrograde flow of actin filaments). Molecules that capture microtubule ends (e.g., IQGAP1) or suppress microtubule instability (e.g., MAP1B) are also potential targets for guidance signals (Dickson 2002).

1.2.3. Scaffolds

Many strategies have been devised to develop three dimensional biomaterials to be used as scaffolds. They have to essentially act as support matrices or templates to assist the growth of cells. Another key feature of advanced scaffolds is their ability to provide structural organization to the cells, which help in their unique architecture and geometry.

1.2.3.1 Features of an ideal scaffold

Scaffolds should be highly porous and providing large surface areas for cell growth and proliferation. They need to be also biodegradable. The degradation rate of the scaffold should be adjusted so as to match the rate of neotissue formation. Furthermore, the degradation products should be non-toxic. They should also possess adequate mechanical strength and have properties that will allow cell proliferation, adhesion, migration and differentiation. The scaffold should provide an environment that facilitates the growth, regeneration and differentiation of the target cells (REF). Structural uniformity in tissue engineering scaffolds is necessary not only for uniform cell distribution, but also for well-controlled material properties. Uniform pore size and distribution ensure diffusion of nutrients into all areas of the gel and the removal of metabolic wastes from the system (Kuo and Ma 2001).

A number of scaffold materials both of synthetic and natural have been tried with regard to neural tissue engineering (Bellamkonda *et al.* 1995). Synthetic materials such as Poly ethylene glycol (PEG) , Poly (ethylene co-vinyl acetate), Poly(glycolic acid) (PGA), poly (lactic acid) (PLA), poly(2-hydroxyethyl methacrylate) (pHEMA-MMA), polypyrroles (Ppys) have all been used as scaffolds for drug delivery(Verreck *et al.* 2005). These various scaffolds have variable properties. Some are biodegradable and some are not. Also, the degradation products of some of these scaffolds increase the pH at the site of the scaffold implantation. They have to be formulated in such a way so as to minimize the immune responses and enhance the mechanical properties.

Polymers from natural sources are particularly useful as biomaterials and in regenerative medicine, given their similarity to the extracellular matrix and other polymers in the human body, chemical versatility as well as typically good biological performance. Owing to their similarity with the extracellular matrix (ECM), natural polymers may also avoid the stimulation of chronic inflammation or immunological reactions and toxicity which is often detected with synthetic polymers (Mano *et al.* 2007).

Various natural polymers such as agarose, alginate, fibrin, collagen, chitosan , dextran etc have also been tried for neural applications(Balgude *et al.* 2001; Lee and Mooney 2001; Amado *et al.* 2008). Since they are obtained from natural sources they should be extensively purified to prevent foreign body response (inflammation, fibroplasias or fibrosis) (Soon-Shiong *et al.* 1991) at the site of implantation. All foreign materials evoke an inflammatory response; however, the goal is to minimize this reaction because a fibrotic scar will often form at the materials–tissue interface, thereby isolating the implanted polymer from the body (Shoichet 2009). When compared to synthetic materials, biopolymers are easily obtainable, and evoke lower foreign response due to their similarity to the host tissue.

1.2.3.2 Hydrogels

Hydrogels are a class of highly hydrated polymer materials with water content of atleast 30 % by weight. These materials are made up of hydrophilic polymer chains, which are either synthetic or natural in origin. The structures of hydrogels are primarily due to the various cross links formed between polymer chains via various chemical bonds and physical interactions. They are typically degradable, can be processed by relatively mild conditions and have mechanical and structural properties similar to many tissues and the extracellular matrix and can be delivered in a minimally invasive manner(Drury and Mooney 2003).

Hydrogels must meet a number of criteria to be of use in tissue engineering and to promote new tissue formation. These parameters include both the physical parameters such as degradation as well as biological parameters like cell adhesion. Also, to be of functional value they should be biocompatible. Biocompatibility basically relates to the material's ability to exist at the site of implantation without eliciting an inflammatory response which may lead to damage to neighbouring cells or leading to significant amounts of scarring thus detouring from its function (Ríhová 2000). Hydrogels are generally regarded as biocompatible due to their relatively high water content and low

interfacial tension with the surrounding environment, as well as their similarity to the highly hydrated macromolecular- based materials in the body. Natural hydrogels have significantly higher biocompatibility when compared to their synthetic counterparts (Lee *et al.* 2000; Lee and Mooney 2001).

Factor release from degradable gels can be tuned by controlling either factor diffusion or gel degradation. Fast degradation will lead to rapid release of growth factors, while slowing degradation will retard factor release and hence by chemically modifying the polymer, the degradation rates can be controlled (Fournier *et al.* 2003). For example, typical alginate hydrogels present a slow and unpredictable degradation *in vivo.* Recent studies have addressed this limitation by partially oxidizing the polymer chains with sodium periodate to enable hydrolytic degradation and modifying the polymer molecular weight distribution (Bouhadir *et al.* 2001; Boontheekul *et al.* 2005).

1.2.3.2.1 Agarose

Agarose is a polysaccharide with alternating copolymers of 1,4-linked 3,6-anhydro-α- L -galactose and 1,3-linked β- D -galactose. It is a marine algal polysaccharide.

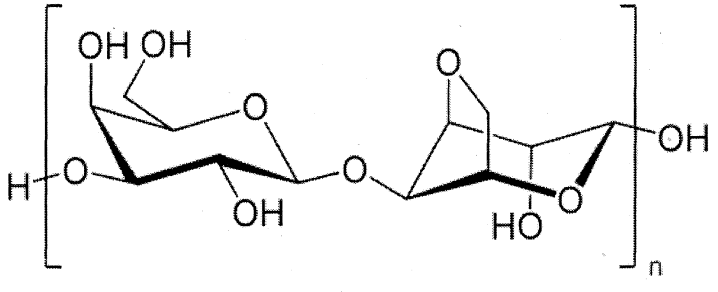

Figure 6. Chemical Structre of Agarose

Low gelation temperature agarose solidifies at 8-17° C and stays solid until melting around 37°C, thus demonstrating a high degree of thermal hysteresis. Agarose is injectable, biocompatible and can be linked with proteins to encourage axonal elongation (Martin *et al.* 2008).The porosity and other physical characteristics of the polymer can be adjusted by varying the concentrations of alginate. Agarose can be made into a scaffold by adjusting its thermodynamic properties (Bellamkonda *et al.* 1995). Another advantage is that one can make variations in the porosity of the scaffolds thus facilitating the controlled delivery of drug molecules from these scaffolds. The large pore sizes and low mechanical stiffness of the gels may enable the migration and proliferation of cells, and these factors can affect the neurite growth as well (Dillon *et al.* 1998). It has been found that low gelation temperature agarose does fostel axonal outgrowth in vitro. However, the low melting point of agarose makes it use difficult in vivo (Balgude *et al.* 2001).

1.2.3.2.2 Alginate

Alginate is the monovalent form of alginic acid and is a linear polymer of β(1->4)-linked D-mannuronic acid and α(1->4)-linked L-guluronic acid, which occurs combined with calcium and other bases in the cell walls and intracellular matrix of brown seaweeds (Drury and Mooney 2003).

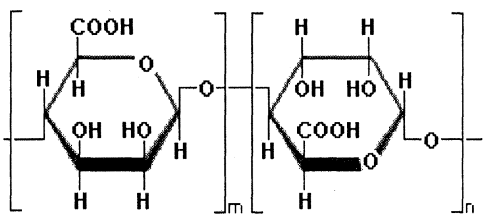

Figure 7. Chemical structure of Alginic acid

The solubility of the polymer in water depends on the type of salts that it froms. Calcium salts of alginate are water insoluble. Cross linking is aided by the presence of

Ca^{2+}. Crosslinking of alginate occurs when its constituent monomers, mannuronic acid (M) and guluronic acid(G), are formed into poly-M , poly-G and alternating MG blocks in the presence of any of numerous divalent or trivalent cations. Ca^{2+} is, by far, the most widely used crosslinking ion; Ca^{2+} -crosslinked alginate is considered to be clinically safe (Reis *et al.* 2006). This property is used for the entrapment of enzymes, drugs, cells and tissue pieces. Conventionally, cross linking is achieved by dropping alginate/cell droplets into a medium containing Ca^{2+} or Ba^{2+} (Manz *et al.* 2004). Since, it is obtained from a natural source; the polymer has to undergo extensive purification before it can be used as a scaffold. In the purified state alginate causes only very limited inflammation making it a highly biocompatible polymer (Klöck *et al.* 1997; Schmidt and Leach 2003) . Alginate, due to its many advantages has been made use of as wound dressing, dental impression and as immobialization matrix. Alginate beads have also been prepared and used for transplantation of chondrocytes, hepatocytes and islets of langerhans to treat diabetes. Characteristics like pore size, degradation rates and release of drug from the structure can be controlled by alginate composition and type. It has various properties which make it suitable to be used in the delivery of different molecules (Gombotz and Wee 1998; Fournier *et al.* 2003).

Inspite of the advantages that alginate presents, alginate poses some disadvantages as well. One of the major disadvantages is the degradation of alginate. This is due to the loss of divalent ions into the surrounding medium thereby leading to the dissolution of alginate. This process is usually uncontrollable and unpredictable. Hence, there is a need for crosslinking alginate to precisely control the mechanical and /or swelling properties of alginate gels (Lee *et al.* 2000).

1.2.3.2.3 Chitosan

Chitosan has been investigated for a variety of tissue engineering applications due to its structural similarities to many naturally occurring glycosaminoglycans. Chitosan is a natural polymer which is positively charged. It is produced by the alkaline deacetylation

of chitin. It is a linear polymer composed of N-acetyl-D-glucosamine and D-glucosamine, which are linked via β-1,4- glycosidic linkages and distributed randomly.

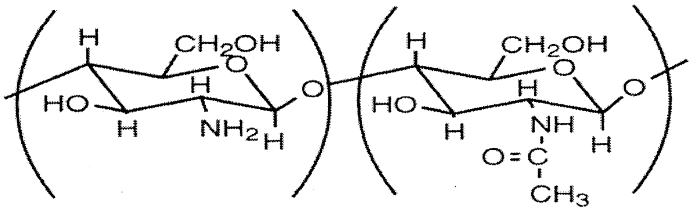

Figure 8. Chemical structure of chitosan

The degree of N-deacetylation usually varies from 50% to 90% and determines the crystallinity, which is greatest for 0% and 100% N-deacetylation. Chitosan is soluble in dilute acids which protonates the free amino groups present. Once dissolved, it can be gelled by increasing the pH or extruding the solution into a nonsolvent. Chitosan derivatives can also be gelled by means of glutaraldehyde crosslinking, UV radiations and by thermal variations. Due to its low toxicity, biodegradability and mechanical properties, it is studied extensively for its use in tissue regeneration(Francis Suh and Matthew 2000; Drury and Mooney 2003).

In vivo studies suggest that chitosan supports axon elongation and improves relevant function. Chitosan by itself has some drawbacks such as limited cell adhesion, proliferation and differentiation of nerve cells. These limitations can be overcome by blending chitosan with other polymers which enhances its mechanical properties and also encourages cell adhesion, proliferation and differentiation of various nerve cell types. Chitosan polymers have improved adhesion properties chiefly attributed to the cationic nature of the scaffold (Zhenhuan Zheng *et al.* 2009). Chitosan polymers also lead to a significantly improved outgrowth of chick Dorsal Root Ganglion (DRG) neurites and better cell adhesion as compared to its attachment on chitin films, which shows that the nerve cell affinity depends on the amino content in the polysaccharide(Freier *et al.* 2005). The in vitro effects of chitooligosaccharide on neuronal differentiation of PC 12

cells was studied and it was found that chitooligosaccharide possesses good nerve cell affinity by supporting the nerve cell adhesion and promoting neuronal differentiation and neurite outgrowth (Yang *et al.* 2009).

1.2.3.2.4 Collagen

Collagen is a main component of extracellular matrices of mammalian tissues like skin, bone, cartilage, tendon and ligament. There are atleast 19 different types of collagen , the basic structure of all of them is composed of three polypeptide chains, which wrap around one another to form a three-stranded helical structure (Lee *et al.* 2001). Physically formed collagen gels are thermally reversible and offer a limited range of mechanical properties. Collagen can be crosslinked with glutaraldehyde or diphenylphosphoryl azide or by physical methods such as UV crosslinking, freeze drying and heating which can significantly improve the physical properties of the collagen scaffold. There has been concern about the cytotoxicity and biocompatibility issues related to glutaraldehyde crosslinked collagens. The cytotoxicity can be minimized by means of neutralization or by using lower concentrations of glutaraldehyde (Glowacki and Mizuno 2008) . However, collagen gels do not have much strength and is potentially immunogenic. The advantage of using collagen is that it meets many of the design parameters and also those specific combinations of amino acid sequences that are recognized by cells and are degraded by certain enzymes secreted by the cells (*i.e.,* collagenase). Collagen has been used both as a scaffold and also as artificial skin due to its ready attachment to various cell types and also its degradation. Furthermore the attachment of various cells to collagen scaffolds can be improved by means chemical modification such as incorporation of fibronectin, chondroitin sulfate or low levels of hyaluronic acid into the collagen matrix. Collagen gels have been utilized in the reconstruction of liver, skin, blood vessels and small intestine(Auger *et al.* 1998; Drury and Mooney 2003).

1.2.3.2.5 Fibrin

Fibrin has been used as a sealant and also as an adhesive in surgery as it plays an important role in the natural wound healing. Fibrin gels can be produced from the patient's blood itself and can be used as an autologous scaffold for tissue engineering. No toxic degradation or inflammatory reactions are expected from the natural component of the body. Fibrin gels by the enzymatic polymerization of fibrinogen at room temperature in the presence of thrombin(Perka *et al.* 2000). An interesting feature of fibrin is the degradation and remodeling by cell-associated enzymatic activity during cell migration and wound healing, and its degradation rate can be controlled by aprotonin, a proteinase inhibitor (Shaikh *et al.* 2008).

Fibrin gels might promote cell migration, proliferation, and matrix synthesis through the incorporation of platelet-derived growth factors and transforming growth factor β. Bidomain peptides with a factor XIIIa substrate in one domain and a bioactive peptide containing RGD sequence in another domain have been covalently incorporated into fibrin gels during coagulation through the action of the transglutaminase factor XIIIa, resulting in gels with potential neurological applications. Fibrin gels have also been utilized to engineer tissues with skeletal muscle cells, smooth muscle cells,and chondrocytes .However, fibrin gels are limited in mechanical strength, and this prevents their use in certain applications (Lee and Mooney 2001).

1.2.4 Alginate based anisotropic capillary hydrogels

Alginate has an inherent ability to form anisotropic capillary hydrogels by the directed diffusion of ions. When an alginate sol gets into contact with gelling ions (electrolyte), the molecules gel immediately by covering the sol with a dense skin or membrane. This membrane is referred to as the primary membrane. Microbeads are produced by dropping small volumes of alginate sol into electrolyte solutions

whereas here the primary membrane is trapping the sol which gets radially transformed into a gel by the diffusing ions (Orive *et al.* 2002).

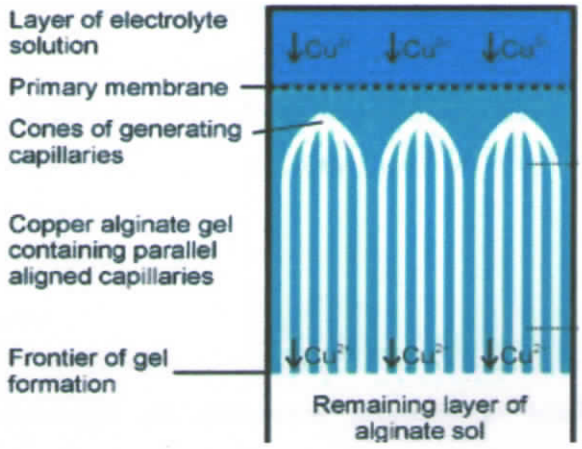

Figure 9. Illustration of different phases of anisotropic capillary gel formation. (Prang *et al.* 2006) The structure is formed after super imposing alginate sol with an electrolyte containing divalent cations

Anisotropic gels with channel-like pores develop when cations diffuse in broad front from one direction into an alginate sol whereas the saccharide molecules get arranged and complexed. Together with the gelation parallel aligned, channel-like pores are formed which can run through the whole length of the gel. Alginate has the capacity to produce capillary hydrogels with multivalent cation solutions like Ba^{2+}, Ca^{2+}, Cu^{2+}, Sr^{2+} and a dilute solution of sodium alginate is superimposed. A membrane like boundary is formed between the interphase which is commonly referred to as the primary membrane. The membrane is non soluble and contains ionically crosslinked alginate. The electrolyte ions start an oriented diffusion into the solution of the polymer, which results into a continuous gel formation process and the generation of capillaries which are hexagonally arranged and are a few centimeters long. The transition from sol to gel is limited by diffusion and proceeds in the propagating front. The lumen of the capillaries is filled with electrolyte solution, while the walls are made up of non soluble metal alginate (Thumbs and Kohler 1996). Anisotropic gels with channel-like pores develop when cations diffuse in broad front from one direction into an alginate sol whereas the

saccharide molecules get arranged and complexed. Together with the gelation, parallel aligned , channel-like pores are formed which can run through the whole length of the gel (Florian Despang 2011). The phenomenon of ionotropic gelation was discovered for alginate leading to a hydrogel with parallel aligned, channel-like pores. Initially, the gelation was carried out mainly with Cu^{2+} which essentially needs to be substituted by either with protons or with a more biocompatible ion such as Ca^{2+} (Prang *et al.* 2006).

1.2.4 Synthetic scaffolds

Synthetic biomaterials are sometimes preferred as scaffolds over natural biomaterials for peripheral and central nerve regeneration both in vitro and in vivo. The advantages of synthetic scaffolds are that there are choices of polymers with various advantages such as biodegradability, biocompatibility, and mechanical properties like the tissue to be replaced. Also , some of them have high porosity which will aid in cell attachment and growth, also the manufacturing process is relatively simple and their chemistry as well as properties are controllable and reproducible. They also have the potential for chemical modification leading to increased interaction with the normal tissue. Several techniques such as nanofiber self assembly, solvent casting and particulate leaching, gas foaming, emulsification ,freeze drying, liquid-liquid phase separation, electrospinning and computer aided design and manufacturing techniques have been employed to fabricate tissue engineering scaffolds with variable amounts of success (Freed *et al.* 1994; Subramanian *et al.* 2009). Synthetic polymers can be reproducibly synthesized with specific molecular weights, block structures, degradable linkages, and crosslinking modes. All these factors contribute to the gel forming dynamics, crosslinking density, and the degradation and mechanical properties of the material.

1.2.4.1 Poly (acrylic acid) and its derivatives

This group contains biomedically important compounds poly (2-hydroxyethyl methacrylate) (P-HEMA), poly (glyceryl methacrylate) (P-GMA) and poly (hydroxypropyl methacrylate) (P-HPMA). One of the most studied synthetic hydrogels is hydrolytically stable cross-linked poly (2-hydroxyethylmethacrylate) (HEMA). The permeability and hydrophilicity of P-HEMA gels could be varied by changing the crosslinking conditions. Poly (HEMA) has been used for developing contact lenses (Kidane *et al.* 1998). P-HEMA gels have also been used for various drug delivery applications.Poly (HEMA) gels are not degradable in normal physiological conditions. Modified poly (HEMA) gels have been synthesized, these dextran modified poly(HEMA) gels are reported to be degradable by enzymes (Stubbe *et al.* 2003).

Gels of poly(acrylamide) (PAAm) and of some N-substituted derivatives of PAAm can be readily prepared by the free radical polymerization of an aqueous solution of acrylamide containing a small fraction of cross linking agent (often N, N-methylenebisacrylamide). These gels are optically transparent, mechanically weak and can have high water content (>95%).

Poly(N-isopropylacrylamide) (PNIPAAm) is exhibits phase transition behavior above the lower critical solution temperature (LCST). The LCST of PNIPAAm in water is approximately 32 °C and can be matched to body temperature by copolymerzation. Another PNIPAAm based polymer, poly (N-isopropylacrylamide-co-dimethyl-γ-butyrolactone acrylate-co-acrylic acid) [poly(NDBA)], was synthesized by radical copolymerization with 7.00 mol% dimethyl-γ-butyrolactone acrylate in tetrahydrofuran. It was found that the LCST of the polymer is between room temperature and body temperature and that takes about 2 weeks for the LCST to surpass body temperature under physiological conditions. The polymer also has relatively low cytotoxicity when studied with 3T3 fibroblast cells (Cui *et al.* 2011).

1.2.4.2 Poly (Ethylene Oxide)

Poly ethylene oxide (PEO) is an FDA approved material for use in various medical applications. It is one of the most commonly used synthetic hydrogel polymers for tissue engineering. PEO and the chemically similar poly(ethylene glycol) are hydrophilic polymers. These polymers can be photocrosslinked by modifying each end of the polymer with either acrylates or methacrylates. When mixed with appropriate photoinitiator and crosslinked via UV exposure, PEO and PEG can form hydrogels (Nguyen and West 2002). Incorporation of the peptide sequence Ala-Pro-Gly-Leu has also been introduced into these gels, which has made these gels susceptible to enzymes existing within the body which makes it friendlier with regard to tissue engineering applications. Various PEO based polymers have been used in drug delivery applications (Lee and Mooney 2001).

1.2.4.3 Poly Vinyl Alcohols (PVA)

Poly(vinyl alcohol) (PVA) is a water soluble polymer formed by the hydrolysis of poly(vinyl acetate). By regulating the hydrolysis and molecular weight of the polymer ,the hydrophilicity and solubility of PVA can be controlled. Cross linking of PVA can be carried out with glutaraldehyde or epichlorohydrin. The chief disadvantage of these hydrogel is that PVA is not degradable in normal physiological conditions. Hence , they can find use most probably as permanent scaffolds. These hydrogels have been used in various tissue engineering applications such as for regeneration of artificial articular cartilage, hybrid-type artificial pancreas and bone-like apataite formation(Taguchi *et al.* 1999; Zheng *et al.* 2009). Incorporation of oligopeptide sequences significantly enhances cellular attachment. After incorporation of a Gly-His-Lys sequence enhanced hapatocyte attachement and the RGDS sequence incorporation has been investigated for corneal

epithelial cell adhesion (Kobayashi *et al.* 1992; Kawase *et al.* 1999; Lee and Mooney 2001).

1.2.4 Scaffolds for neural tissue engineering and axonal guidance

A cellular scaffold used for tissue stimulation is called a superstructure. There are many ways to form synthetic superstructures. These include the use environmental stimuli such as heat or the formation of ordered longitudinal channels or fibers, and also tensile axons and nanofibrous structures (Biazar *et al.* 2010).

1.2.4.1 Longitudinally oriented guides

Longitudinally oriented channels are structures that could be added to a generating conduit in order to give the regenerating axons. The longitudinal channels act as well defined guide for the axons to grow straight through. Following axonal damage or injury, the regenerating axons are able to extend through open longitudinal channels which mimic the endoneural tubes within the peripheral nerves. Also, the presence of longitudinal channels adds the advantage of increasing the surface area available for cell contact. The desirable structure would have multiple longitudinal channels within the same scaffold. Directionally oriented anisotropic channels could be created in scaffolds by chemical processes. Such structures were created by the orderly migration of copper ions through sodium alginate solution when the alginate solution was superimposed with the electrolyte solution (Pawar *et al.* 2011). Also, the channels could be molded into the scaffold. Wang *et al.*, devised an innovative molding technique was developed and used to produce inner matrices with multiple axially oriented macrochannels and radially interconnected micropores. Acupuncture needles were used as mandrels during molding to improve the safety and controllability of the process. The in vitro cell culture experiments using this innovative scaffold showed that the differentiated neuro-2a cells grew along the oriented macrochannels and the interconnected micropores which was

beneficial for the nutrient diffusion and also for cell ingrowth to the interior of the scaffold (Wang *et al.* 2006).

Another method to create desirable longitudinally oriented channels is to create a conduit from one polymer with embedded longitudinally oriented fibers from another polymer, and then selectively dissolve the fibers to form longitudinally oriented channels. In a study conducted by Yu *et al.*, HEMA 2-hydroxylethyl methacrylate was copolymerized with ethyl methacrylamide (AEMA) to create a P(HEMA-co-AMEA) gel. PCL fibers were embedded in the gel, and then selectively dissolved by acetone with sonication to create channels. It was found that HEMA in a mixture with 1% AEMA created the strongest gels. The scaffolds were then modified with peptides and they could be easily fabricated in aqueous conditions, highly reproducible, well-defined, and enhanced neural cell adhesion and guided neurite outgrowth of primary chick dorsal root ganglia neurons relative to the non-peptide modified controls(Yu and Shoichet 2005).

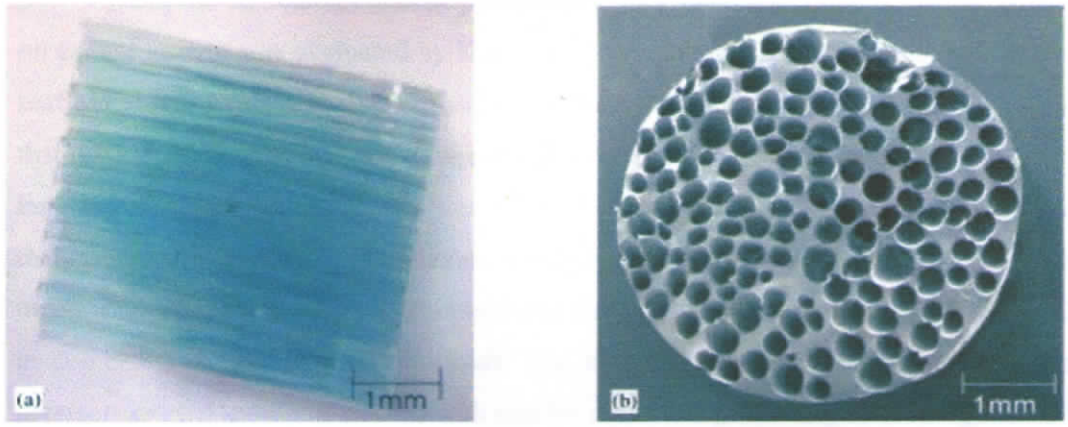

Figure 10 . A transparent P(HEMA-co-AEMA-1%) scaffold: a) stained with 0.4% Giemsa methanol and viewed by a longitudinal cross section by light microscopy and (b) a horizonatal cross-section of the same scaffold viewed by SEM had a mean deviation of 132± 5 channels (Yu and Shoichet 2005)

4.2.2 Copper capillary alginate scaffold

The capillaries in copper aliginate scaffolds showed an uniform distribution with a diameter ranging from 16μm to 80μm (Figure 14 a-d). The average capillary diameter of the upper, lower and middle regions of the scaffold (Figure 15) suggested that there are variations in diameter as the capillaries develop deeper into the scaffold region. Besides, the parallel nature of capillaries were highly reproducible (Figure 14 c, d) in each batch synthesized. It was found that the average capillary diameters varied significantly from each other for all the samples from different batches. This maybe either due to the fact that the cross linking ion within a given gel are not consistent or there is significant error that is involved in the sample sectioning, the latter being the most suspected case. The major difficulty in sectioning was removing the upper region of the gel, which had varying thickness among the batches. This variation had significant effect on the diameter of the capillaries. Options like keeping the copper solution levels and alginate in a constant level did not helped in formation of predictable capillaries with same diameter. Since the capillaries showed a tapering effect as the depth increases, we decided to take the middle most sections of the scaffolds with an average diameter of approximately 33 μm which had more capillaries of uniform, dimensions.

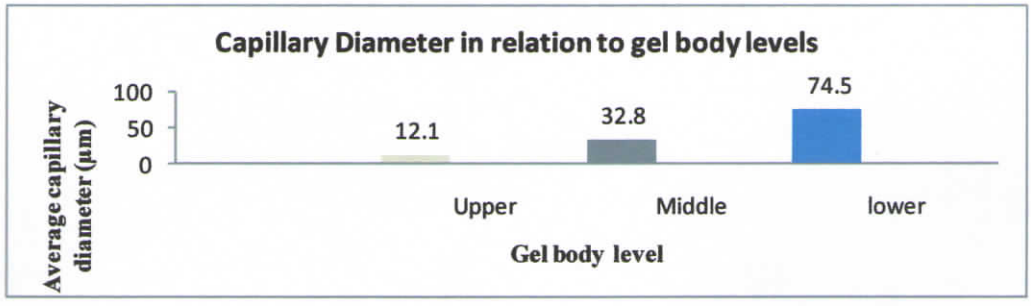

Figure 15. Graph showing capillary diameter in relation to the gel body levels. The Upper gel sections showed thinner capillaries with an average diameter of (12.1μm), the middle section showed uniform distributions of pores with a uniform diameter of 61.7μm and the lower section showed an average pore diameter of 92.3 μm.

1.2.4.2 Longitudinally oriented fibers

Longitudinally oriented fibers can also be added to a conduit to provide regenerating axons with guidance for longitudinally directed growth. It has been shown that adding filaments to a scaffold promotes inner contact guidance and also helps in increasing the permeability for better nutrient and waste exchange. A novel synthetic scaffold comprising collagen crosslinked with a terpolmer of poly(N-isopropylacrylamide) (PNiPAAm) as conduits for nerve growth. The authors could demonstrate that neuronal growth could be enhanced on the collagen-TERP scaffolds through the incorporation of the support fibers. Neuronal growth on these matrices were evealuated by using isolated dorsal root ganglia as a nerve source. It was found that the incorporation of fibers into the collagen-TERP scaffolds produced a significant increase in neurite extension(Newman *et al.* 2006).

Also, the combined effect of permeable PLA conduits and microfilament bundles on axonal growth was evaluated by Kai *et al.* The results demonstrated that the filament scaffold enhanced tissue cable formation and Schwann cell migration. It was also found that the scaffold enhanced axonal regeneration towards the distal stump, especially along long lesion gaps , but significance was obtained only using PLA conduits. They observed that when compared to the silicone conduits, permeable PLA conduits enhanced myelinated axon regeneration across both the lesion gaps and achieved significance only in combination with filament scaffolds. The microfiber guidance characteristics were inversely related to fiber diameter, with smaller diameters promoting better longitudinally oriented cell migration and axonal regeneration (Cai *et al.* 2005).

1.2.4.3 Oriented matrices

It has been shown that *in vivo* experiments with oriented matrices have a higher growth value than ionotropic matrices of the same material. Various cells recognize a three-dimensional geometrical structure on the surface of substrates, and their growth can

be guided and controlled by fabricating microgrooves on substrate surfaces. The cells exhibit sensitivity to the dimensions of the microgrooves.

Most of the microgrooves have been fabricated on inorganic substrates, such as micromachined silicon chips which are not very desirable for implantation. Micropatterned regions on glass coverslips with adsorbed laminin have been demonstrated to provide chemical guidance for axonal outgrowth(Tai and Buettner 1998).

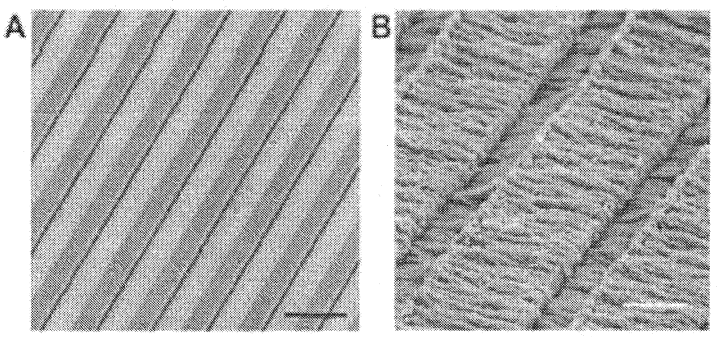

Figure 11 Schwann cells on smooth compression-molded poly-D, L-lactic acid substrate biomaterials (Tai and Buettner 1998)

The magnetic alignment of positive or negative diamagnetic anisotropic molecules, such as fibrin and collagen respectively, elicit guided in vitro regeneration and improved in vivo regeneration(Tai and Buettner 1998; E. Biazar 2010).

1.2.4.3 Topography and design considerations for axonal growth and guidance

The three main levels of scaffold structure include nanostructure, microstructure and the superstructure. These three hierarchical levels should be considered while designing a scaffold. The term superstructure basically relates to the overall shape and dimension of the scaffold. The microstructure refers to the cellular level structure and the

nanostructure relates to the subcellular level. Both physical and chemical cues can be used for directing cell growth on scaffolds (Norman and Desai 2006).

1.2.4.3.1.Chemical cues

Chemical cues can be used to create topography by selectively depositing polymer solution in patterns on the surface of a substrate (Kam *et al.* 2001). There are different methods for depositing the chemical cues. Two methods for dispensing chemical solutions include stripe patterning and piezoelectric microdispensing.

a) Stripe-patterned polymer films

They can be formed on solid substrates by casting diluted polymer solution. The method is relatively easy, inexpensive, and has no restriction on the scaffold materials that can be used. The procedure involves horizontally overlapping glass plates while keeping them vertically separated by a narrow gap filled with a polymer solution (Norman and Desai 2006).

Tsuruma *et al.*, in 2006 prepared a regular stripe-patterned (groove-ridge pattern) polymer film by self-organization for controlling the direction of neurite extension. Neural cells from cerebral cortex of embryonic 14- day old mice were cultured on a poly-l-lysine coated film. The authors have described a complex and unusual contact guidance dependent on the pattern feature size. The neurites grew perpendicular to wide groove of 12.7 μm and wide ridge of 4.3 μm but parallel to narrow grooves (6.1 and 8.4 μm) and narrow ridge (2.2 and 3.6 μm). The neurites sprouted parallel to the narrow groove but uniformly on the wide groove. The emersion of neurites was suppressed and the length of neurites was longer compared with on a flat film (Tsuruma *et al.* 2006).

b) Microdispensing

This method is used to create micropatterns on polystyrene culture dishes by dispensing droplets of adhesive laminin and non-adhesive bovine serum albumin (BSA) solutions. The microdispenser is a piezoelectric element expands when voltage is applied,

causing liquid to be dispensed through the nozzle. The microdispenser is moved using a computer-controlled x-y table. The micropattern resolution depends on many factors: dispensed liquid viscosity, drop pitch (the distance between the centre of two adjacent droplets in a line or array), and the substrate. With increasing viscosity the lines become thinner, but if the liquid viscosity is too high the liquid cannot be expelled. Heating the solution creates more uniform protein lines. Although, some droplet overlap is necessary to create continuous lines, uneven evaporation may cause uneven protein concentration along the lines; this can be prevented through smoother evaporation by modifying the dispensed solution properties (Laurell *et al.* 1999).

Gustavsson et al., in 2007 developed a microdispenser technique in order to create protein patterns for guidance of neurites from cultured adult mouse dorsal root ganglia (DRG). The developed microdispenser could eject 100 picolitre droplets and could also position the droplets with a precision of 6–8 μm. Laminin and bovine serum albumin (BSA) was used to create adhesive and non-adhesive protein lines on polystyrene surfaces (cell culture dishes). Whole-mounted Dorsal Root Ganglia (DRG) was then positioned close to the patterns and neurite outgrowth was monitored. The neurites preferred to grow on laminin lines as compared to the unpatterned plastic. When patterns were made from Bovine Serum Albumin (BSA) the neurites preferred to grow in between the lines on the unpatterned plastic surface. The authors conclude that microdispensing can be used for guidance of sensory neurites (Gustavsson *et al.* 2007).

1.2.4.3.2 Physical cues

Physical cues can significantly influence cellular organization on culture, this is referred to as contact guidances (Rajnicek *et al.* 1997). Physical cues can either result in ordered or unordered topographies.

1.2.4.3.2.1 Oriented topographies

The ordered topographies consist of patterns which are highly organized and geometrically precise. Creating such topographies is quite tedious (Norman and Desai 2006).Some of the methods to create such oriented and directed topographies on a scaffold include

a) Photolithography

This method involves exposing a photoresist-silicon coated wafer to a light source. The desired pattern is created by placing a mask with the pattern in between the light source and the silicon coated wafer. This allows the light to filter through the mask and create the desired pattern on the photoresist wafer. This method when performed near the UV range is often viewed as a standard for fabricating topographies on the micro level (Sorribas *et al.* 2002). Grooved substrata of different pitches and depths, patterned photolithographically, have been used to assess the extent to which topographical cues alter the direction of neurite growth (Rajnicek and McCaig 1997). When grown on top of narrow, shallow grooves (1–4 mm wide and 14–1100 nm deep), neurites orient parallel or perpendicular to grooves depending on cell type (Rajnicek *et al.* 1997).

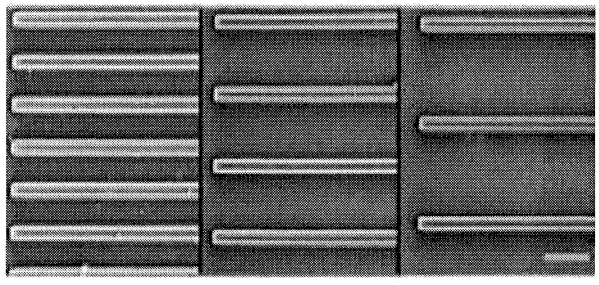

Figure 12 Scanning electron micrographs of microchannels. Polyimide walls 10 mm wide, 11 mm in height, and 400 mm in length were prepared on glass slides using standard photolithographic techniques. Walls were spaced 20–60 mm apart to form microchannels of

different width: 20 mm wide (left), 40 mm wide (middle), and 60 mm wide (right) (Mahoney *et al.* 2005).

Mahoney *et al.*, in 2005 created microchannels using a photolithographic technique to pattern polyimide walls (11μm in height and 20-60μm in width) onto a planar glass substrate. PC 12 cells were seeded onto these patterned surfaces. It was observed that after 3 days of culture in NGF supplemented medium the cells were viable and extended neurites. Also, the culture in microchannels influenced the direction of neurite growth and the complexity of PC 12 cell architecture including neurite length and number of neurites emerging per cell. Within the microchannels neurites oriented parallel to channel walls and the complexity of neuronal architecture was found to be reduced. These effects were strongest for cells located in channels 20-30μm wide. by manipulating the channel width the overall direction of neurite growth and complexity of neuronal architecture was controlled (Mahoney *et al.* 2005).

b) **Electron Beam Lithography**

This is an electron-sensitive resist is exposed to a beam of high-energy electrons. There is a choice between positive or negative type resist; however, lower feature resolution can be obtained from the negative resists. Patterns are created by programming the beam of electrons for the exact path to follow along the surface of the material. The resolution is affected by various factors such as electron scattering in the resist and backscattering from the substrate (Gadegaard *et al.* 2007). This method can create a single surface features on the order of 3-5 nm. If multiple features are required over a larger surface area, as is the case in tissue engineering, the resolution drops and features can only be created as small as 30-40 nm, and the resist development begins to weigh more heavily on pattern formation. To prevent dissolution of the resist, ultrasonic agitation can be used to overcome intermolecular forces. In addition, isopropyl alcohol (IPA) helps develop high density arrays (Bhatnagar *et al.* 2006; Norman and Desai 2006).

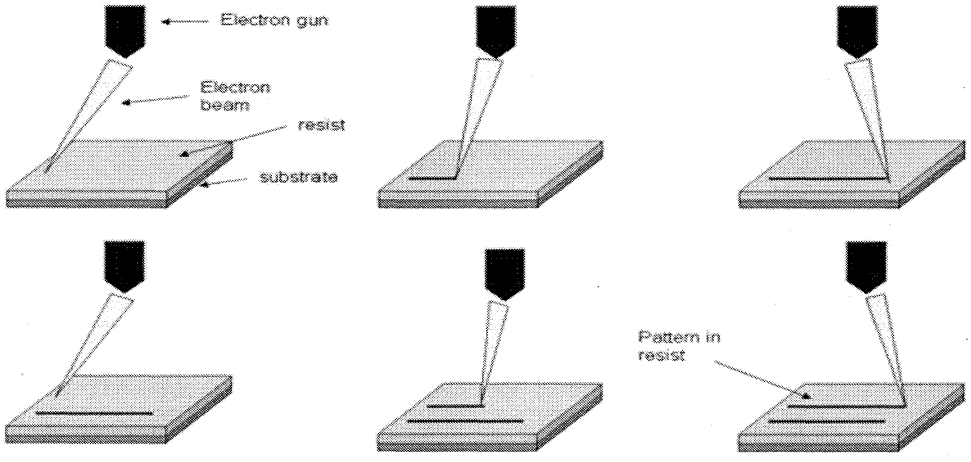

Figure 13 : Schematic diagram of electron beam lithography process. A computer controlled electron gun scans the an electron beam across the resist-coated surface creating the preprogrammed pattern.(Norman and Desai 2006)

Gomez *et al.*, in 2007 investigated how neurons behaved on poly(dimethyl siloxane) (PDMS) surfaces decorated with biochemical and physical cues presented individually or in combination. In particular, nerve growth factor (NGF) was covalently tethered to PDMS to create a bioactive surface, and microtopography was introduced to the material in the form of microchannels. Embryonic hippocampal neurons were used to investigate the impact of these surface cues on polarization (i.e., axon initiation or axogenesis) and overall axon length. It was found that topography had a more pronounced effect on polarization (68% increase over controls) compared to immobilized NGF (27% increase). In addition to axon formation, chemical and physical cues are also involved in axon growth following the initiation process. Interestingly, for the same studies described above, the effects of microchannels and NGF were opposite from the effects on polarization; the most evident effect was for the immobilized growth factor (10% increase in axon length with respect to controls) whereas there was no effect in general for the microtopography. More importantly, when the two surface stimuli were presented in combination, a synergistic increase in axon length was detected (25% increase with respect to controls), which could be a result of faster polarization triggered by topography plus enhanced growth from NGF. Additionally, axon orientation was also analyzed and

we found the well-known tendency of perpendicular or parallel axonal alignment to be dependent on the width and depth of the channels(Gomez *et al.* 2007).

c) X-ray lithography

This method can form ordered patterns which could be potentially used to investigate the role that topography plays in promoting neuritogenesis. The mask parameters determine the pattern periodicity, but ridge width and depth are determined by the etching conditions. In a study by Foley *et al* in 2005 patterned surfaces were made by x-ray lithography and *it* was found that the threshold for induction of neuritogenesis was markedly reduced when cells were cultured on ridges of 70 and 250 nm. In contrast, contact guidance of neurites was independent of feature size. These results suggest that the scale of topographic features can act cooperatively with NGF signaling to regulate the formation of neurites. These findings may have general relevance to differentiation processes in neurons as well as in other cell types (Foley *et al.* 2005).

1.2.4 Models for studying axonal growth and guidance

A major challenge in neurobiology is to understand the basic mechanism underlying axonal growth and guidance. For studying the underlying principles governing these phenomena it is necessary to have model systems. The most relevant model systems for studying axonal growth and guidance would be perhaps primary neurons or a continuous clonal cell line.

1.2.4.1 Primary neurons

Primary neuronal cultures are prepared from cells directly taken from the animal. Primary neurons are preferred over continuous (clonal) cell lines from the CNS, as they have the capability to form well defined axons or dendrites and can establish functional synapses. In principle, primary nerve cell cultures could be prepared from any region of

the brain or spinal cord (Kaech and Banker 2006). The situation with culture of neurons when compared with other tissues is quite different. When cells from the embryonic brain are dissociated and plated in culture, neurons that have completed division in situ will extend processes, form synapses and become electrically active. But if the tissue is removed at a time of active neurogenesis, it is quite rare to observe cells that divide in culture and subsequently acquire a neuronal phenotype. This makes the culture of neurons fundamentally different. The primary neuronal cells divide or not, depending on their their stage whether of embryonic origin or not , acquire differentiated characteristics – and ultimately die..Their passaging frequency is very low. For the next experiment one has to go back to the source again to prepare new cultures (Banker and Goslin 1998).

1.2.4.2 Pheochromacytoma -12 Cell Line

The Pheochromacytoma-12 (PC12) cell line has been used as a model cell line for the investigation of neuronal differentiation in vitro. PC12 cells originate from chromaffin cells, whose differentiation into sympathetic neurons can also be induced by some factors like NGF, bFGF and cAMP (Sofroniew *et al.* 2001).

When the PC12 cell line is exposed to Nerve Growth Factor (NGF), the cells respond by ceasing cell division and extending neurites (Greene and Tischler 1976) and this is accompanied by the induction of electrical excitability, sensitivity to acetylcholine, and an increase in the specific activity of choline acetyltransferase (Dichter *et al.* 1977; Schubert *et al.* 1977; Gunning *et al.* 1981). PC12 cells exhibit many phenotypical characteristics associated with pheochromacytoma cells and their non neoplastic counterparts, adrenal chromaffin cells. They synthesize, store, release (in response to secretagogues and depolarizing agents), and take up considerable levels of catecholamines (Greene and Rein 1977). The PC12 cell line also manifests many features of sympathicoblasts- the cells that give rise to postmitotic sympathetic neurons (Banker and Goslin 1998). In the unstimulated state, these cells are round, projecting a few

filopods but no neurites or growth cone like structures. Upon stimulation with NGF, they project neurites tipped by small growth cones. Both the cell body and the growth cones respond to NGF initially with membrane ruffling, an event that involves actin polymerization (Bearer 1992). The PC12 rat pheochromacytoma cell line has been used extensively to study various problems related to neuronal differentiation and function. This widespread usage of the cell line is attributed to the homogeneity, relative stability, high degree of differentiation and of differentiative capacity. Its robust response to NGF and dramatic change in phenotype brought about by this factor, fidelity to many of the features of normal neuroblasts and neurons poses great potential for genetic manipulation and the accrual of a large number of studies regarding its characterization (Banker and Goslin 1998). Also, it has been found that they form synapse like structures (Jeon *et al.* 2010). It has been found that PC 12 cells form typical synapses with neurons in primary culture when PC12 cells are differentiated by NGF are seeded into primary neuron cultures (Zhou *et al.* 2006).

1.3 Hypodissertation

Regeneration within the Central Nervous System (CNS) does not occur spontaneously. The field of neural tissue engineering investigates the cues that can be provided to overcome the inhibitory environment prevailing within the CNS. Neurons, both in the *in vitro* and *in vivo* conditions navigate complex environments by integrating a variety of cues, including indiffusible factors; substrate bound factors, electrical and magnetic fields and also the topographical features. A number of studies have suggested that pre-formed pathways of differential adhesiveness are crucial in guiding neuronal growth cones to distant targets *in vivo*. Structural and chemical cues play crucial roles in promoting neuronal growth, neurite extension and thereby helping in neuronal pathfinding. Since this is a complex process, involving a series of proteins both within the cell as well as on the plasma membrane, it is essential to have a model system in which multiple axons grow though predefined channels within scaffolds so that cellular events can be studied easily. Towards the goal, in this study I focused on the development of an anisotropic copper capillary alginate scaffold with oriented tube like pores. Essential roles for such a scaffold should include biocompatibility, parallel channel formation and also allow axons to attach and grow to a defined length. In addition to the above, itwould be an added advantage if these scaffolds allow the incorporation of growth factors like neuronal growth factor and transformation growth factor.

1.4 Objectives

The main objectives of this work were

1. Determine if anisotropic capillaries could be created within alginate by the directed diffusion of divalent ions.
2. Stabilization of the scaffold.
3. Optimization and characterization of the capillary alginate scaffold.
4. Determining the biocompatibility of the scaffold.

Materials and Methods

Chapter 3

Materials and Methods

3.1 Materials

Sodium alginate with a viscosity of > 2000 cps (2% aqueous solution, 25° C) from SD Fine Chem limited, India and Sigma Aldrich, USA; Copper Nitrate from Merck, India; Hexamethylene diisocyanate (HDI > 99%) from Sigma Aldrich, USA; Acetone extrapure AR from Sisco Research Laboratories, India were used.

DMEM was obtained from Gibco, Germany and Hams F12 from Himedia, The complete cell culture media was supplemented with 10% Horse Serum (PAN, Germany) and 5% Fetal Bovine Serum (PAN, Germany). The media also contained 100 U / ml of Penicillin G (Sigma Aldrich) and Streptomycin (Gibco, Germany) and Sodium bicarbonate, Sisco Research Laboratories, India. Poly- l-lysine hydrobromide, Sigma Aldrich, and Collagen from rat tail , Bornstein and Traub Type I (Sigma Aldrich) to enhance PC 12 attachment. Nerve growth factor -7 S (Sigma Aldrich) was used for the differentiation of PC 12 cells. Live dead Cell assay kit (Molecular probes, Invitrogen) was used for determining the cell viability.

3.2 Methods

3.2.1 Alginate Gel formation

Sodium alginate was dissolved at a concentration of 2 g / 100 mL (2% w/w) in purified water. Electrolyte solutions copper nitrate (Cu (NO_3)) and Calcium chloride ($CaCl_2$) was prepared at a concentration of 1 mol/L in purified water. The electrolyte solutions were subsequently filtered through vacuum filtration system equipped with a membrane of pore size of 0.2 μm (PALL Life Sciences, Germany).

3.2.1.1 Spray method

65 mL of alginate solution was poured into a glass measuring cylinder (2.5 cm in diameter and 10 cm in height). It was allowed to stand for about 2 hours; the alginate molecules should get close contact with the hydrophilic walls of the mould which is important for the stability during gel formation. Then the electrolyte solution was sprayed onto the alginate solution using a spray bottle until the alginate was covered by a 5 mm thick layer of electrolyte solution (~10 mL); after several minutes another 10 mL of electrolyte solution were filled onto the alginate using a pipette. The moulds were covered by a lid and allowed to stand for at least one day until gel formation was finished. With the help of a spatula the metal alginate gels were carefully removed from the moulds and immersed in sterile filtered water to remove excessive electrolyte; the water was changed after at least 4 hours for not less than 4 times (Prang *et al.* 2006).

3.2.1.2 Alginate gel preparation in petri plates

A thin coat of alginate was first baked onto the glass petri dish walls to prevent the alginate gel separating from the dish during the capillary growth. Three thin coats of alginate solution was smeared onto the onto the entire inner surface and rim of a Borosil petri dish (5 cm diameter × 1.7 cm height) petri dish surface and baked using a microwave oven. After each application of alginate coating, the dish was allowed to air dry and then baked in the oven. This procedure was done for 3 additional times.

The alginate coated petri dish was carefully filled to the top, almost overflowing with freshly prepared 2 % w/v sodium alginate solution. A sheet of tissue paper was first soaked in the electrolyte (Copper nitrate or Calcium chloride, as the case maybe) and was stretched taut and placed carefully directly on top of the alginate filled petri dish. The entire surface of the alginate solution should be in good contact with electrolyte soaked tissue paper. After which, 1-2 mL of the electrolyte solution was

added carefully to the tissue paper using a pipette. The tissue paper is gently peeled off the alginate surface without disturbing the hydrogel. A solid membrane, contiguous with the rim of the petri dish approximately 1 mm thick completely covered the top of the alginate-filled petri dish. The primary membrane appeared to be a little tough. Taking extreme care not to jar the gelling solution, the filled petri dish was transferred to a 1 L glass beaker. The electrolyte solution is then carefully pored along the sides of the beaker such that it allows a 1.5 to 2 cm submersion of the petri dish. The dish was then left undisturbed for 24 hours at room temperature (Willenberg *et al.* 2006).

3.2.1.3 Gel cutting

The obtained gel bodies were cut perpendicular to the longitudinal axis of the capillaries using a sterile scalpel blade. The non-structured top layer of the gel (5 mm) one slice of 15 mm thickness was cut from the gel cylinder.

3.2.1.4 Dehydration, crosslinking and ion exchange

Gel slices were dehydrated by equilibrating in acetone/water mixtures of rising acetone content (25%, 50%, 75%) for a minimum of 4 hours per step; then the gels were equilibrated in pure acetone and then in dry acetone twice for not less than 4 hours per step; solutions are slightly agitated by stirring. Hexamethylene diisocyanate (HDI) was dissolved in dry acetone at a concentration of 0.1 mol/L and dehydrated acetone-soaked alginate gels were immersed in HDI solution for 4 hours under slight stirring. Gels were removed from HDI solution and immersed in dry acetone for 5 min to remove HDI from the capillary lumens. Then the gel slices were put between two filter papers and dried in air for 10 minutes to remove acetone from the capillary lumens. The gels were immersed in sterile filtered water (with a load from the top because gels are swimming on the water interface) for 4 hours under slight stirring. Then they were heated in water to 70°C for additional 2 hours until carbon dioxide development stopped. After that, the gels were immersed in 1 mol/L

hydrochloric acid solution (HCl) five times for at least 2 hours under slight stirring to remove the crosslinking divalent cations. Finally, the gels were immersed in sterile filtered water for several times until the water reached a neutral pH. Gels were sterilized by incubation in 70% ethanol for 5 minutes and finally kept in sterile phosphate-buffered saline (PBS; pH 7.4).

3.2.2 Characterization of alginate hydrogels

3.2.2.1 Pore structure

Blocks of alginate hydrogels (5 mm x 5 mm x 15 mm) were cut from the gel cylinders using razor blades. Images of the capillary structure were captured using IX 51 inverted microscope (Olympus, Japan), a Rolera-XR Mono Fast 1394 Video Camera (Q Imaging, Canada), and NIS elements software, Advanced Research Version 3.06, (Nikon,Japan).

3.2.2.2 Hydrolysis/Degradation

Mass degradation of raw and cross-linked copper alginate scaffolds was measured for a week's period. Twelve dry scaffolds were weighted and then immersed in PBS (pH=7.4).

3.2.2.3 Scanning electron microscopy

Acetone washed and dehydrated samples of the copper capillary alginate scaffolds produced previously were mounted separately onto aluminum scanning electron microscopy sample stubs with double-sided carbon. The samples were analyzed using, scanning electron microscope equipped with energy dispersive spectroscopy (EDS) system and analyzed with the help of XT software (FEI Quanta EDAX Inc, NJ). The samples were analyzed at 15 KeV accelerating voltage and were sufficient enough to observe the X-ray peaks of interest with EDS.

3.2.2.4 Micro-CT Imaging

The scaffolds were scanned using a cone-beam high-resolution micro-CT 40, (ScanCo Medical AG, Switzerland). The X-ray source was set at 45 kV of X-ray accelerating voltage and 177 μ A of current. Approximately 300 slices were acquired. Each scan took approximately 32.5 minutes. Data sets were reconstructed using standardized cone-beam algorithm based reconstruction software, ScanCo Medical analysis. A standardized threshold value of 60 to 1000 grey level was applied. Structural parameters (pore size, porosity and wall thickness) were calculated in three dimensions from the binarized images.

3.2.2 Cell culture studies

3.2.2.1 HEK-293 cell line

Human embryonic kidney-293 cell line is maintained in Dulbecco's modified Eagle medium supplemented with sodium carbonate, 5% fetal bovine serum , streptomycin and penicillin G. The cells have a spindle morphology are passaged and split to new T-25 flasks or cryopreserved.

3.2.2.2 PC-12 cell line

3.2.2.2.1 PC 12 cell line maintenance

PC12 cells were grown in DMEM Ham's F12 medium with 20 mM HEPES pH 7.4. The culture medium was supplemented with 5% fetal bovine serum serum, 10% heat-inactivated horse serum, 100 IU/ml penicillin, and 100 μg / ml streptomycin (all from Gibco). Cells were seeded in 25 cm^2 flasks at a density of $5x10^5$ cells / flask and subcultured in 6 well plates at a density of 5 $x10^4$ cells / well. The 6 well plates

(Costar, Axygen) were coated with 5 μg/cm^2 poly-L-lysine (Sigma Aldrich). The culture medium was changed every 2-3 days. The experiments were performed 3-8 days after subculture. The cells are round in suspension and on attachment tend to aggregate forming clumps. Cells on reaching 70-80% confluency are passaged in desired ratios to new T-25 flasks or cryopreserved.

3.2.2.2.2 NGF Differentiation of PC-12 cells

The procedure for inducing differentiation in PC12 is given by Greene and Tischler, 1976. 6 well culture plates were coated with Poly-l-lysine to enhance the attachement of the cells. 1.5 ml of Poly-l-lysine was added to each well of the 6 well plate. The culture plates were then placed in humidified condition containing CO_2 incubator (Forma Direct Heat, Thermo scientific) with 5% CO_2 and 37° C. PC 12 cells (10,000 cells/cm^2) were seeded on the PLL coated dishes in 2 ml DMEM F12 complete (10% Horse serum, 5% Fetal calf serum, 1% Penicillin- streptomycin) with Nerve Growth Factor- 7S (50 ng/mL). Cells were maintained for 5-6 days until the neurites were long enough (Greene and Tischler 1976).

3.3 Scaffold cytotoxicity study

3.3.1 Extract preparation of scaffold

Scaffolds (1.25 cm^2 / mL) were incubated in culture medium for 24 hours and 7 days at 37°C with constant shaking (60 rpm) in order to simulate closely the effect of the degradation products in a dynamic environment. The extract was then filtered (0.2 mm pore size) to eliminate any solid material particles and maintained at -20°C. For the extraction tests, complete culture medium in TCPS served as the negative control and 20 mg / mL phenol 99+% in the media served as the positive control.

3.3.2 Live dead assay

Ethidium bromide (Ethidium bromide homodimer-1., Molecular probes, Invitrogen) was used to assess the viability of PC 12 cells following transfection. 2mM Ethidium bromide stock and then diluted with PBS to get a working concentration of 4 μM. 130 μL of the working solution of the stain was added to the plate containing PC 12 cells to which the scaffold extract had been previously added and incubated for 24 hours. It was then incubated for 40 minutes. Ethidium bromide enters the cells possessing membrane damage and emits fluorescence when bound to the nucleic acids. The fluorescence was observed with a fluorescent microscope (IX 51,Olympus) at ex/em~ 495 nm /~635 nm.

3.4.2 Preparation of Competent Cells

Calcium chloride method was used to prepare competent DH5α bacteria. On day one, an LB-agar plate (without Ampicillin) with an inoculated loop full of DH5α was prepared, and kept at 37 °C for 12-16 hours. On the second day, 2 ml LB (without any antibiotic) was inoculated with a single colony of DH5-α and further allowed to grow overnight by incubating at 37 °C. On day three, 2 ml cells were inoculated into 100 ml LB (without antibiotic) at 37°C /300 rpm. To monitor the growth of the culture, the OD600 was determined at very 20-30 minutes until the value was between 0.4 and 0.5.

Once the desirable O.D value was reached, the bacterial cells were aseptically transferred to sterile, disposable, ice-cold 50ml polypropylene tubes. Then, cells were pelleted by centrifugation at 1600 g for 10 minutes at 4 °C. The supernatant were decanted and the pellet was resuspended in 10 ml of 0.1 M $CaCl_2$ (cold) , kept on ice for 10 minutes and centrifuged at 1100 g for 10 minutes at 4 ° C. Pellet was further resuspended in 2 mL of 0.1 M $CaCl_2$ and stored in ice at 4C till use (can be stored

upto a maximum of 7 days). The competent cells can be stored in Dimethyl sulfoxide (DMSO) in -80°C for 2 months. For this , the competent cells were mixed with 75 µL DMSO, mixed well and kept on ice for 15 minutes. Again another 75 µL DMSO was added, mixed well and stored in -80° C as 500 µ L aliquots.

3.4.3 Bacterial Cell Transformation

For transformation, the DH5α cells stored at -80 °C were thawed on ice for 10 minutes. 1 µl (about 10-50 ng) of plasmid DNA (pEGFP-C1) was added to each eppendorf tube with 50µL of the DH5- α competent cells and then kept on ice for 15 minutes, after which the tubes were transferred to 42°C (Thermomixer Comfort, Eppendorf) for 90 seconds. The tubes were then immediately chilled on ice and for 2 minutes. Then, 950 µL of LB broth was added to the mixture. The tubes were then kept in the thermomixer at 37°C with gentle shaking (300 rpm) for 60 minutes. The transformed cells (100 µl) were aspirated and transferred to a LB agar medium plate (containing Ampicillin 50 µg/ml). Transformed cells were gently spread by using a sterile bent glass rod which is first dipped in ethanol and flamed. A negative control with ampicillin and a positive control with LB (no ampicillin) are kept to check the transformation efficiency and rule out contamination. The plates are then incubated overnight at 37°C.

3.4.4 Alkaline Lysis Mini Plasmid Preparation

Mini plasmid preparation of pEGFP-C1 from DH5-α cells was performed according to the alkaline lysis method ((Sambrook and Russell 2001))

1.5 mL of the overnight culture of the transformed pEGFP-C1 DH5α cells was transferred to a microcentrifuge tube. The tube was then centrifuged at 10,000 rpm for 2 minutes at 4° C to pellet the bacterial cells. The supernatant was decanted and then the pellet was carefully resuspended in 375µL of STE buffer by vortexing. The tube was then centrifuged at 10,000 rpm for 2 minutes at 4° C. The supernatant was

removed and the pellet was resuspended careful in 100 µL GTE buffer (alkaline lysis solution I) by vortexing. The tube was then kept at room temperature for 5 minutes. Then, 200 µL of alkaline solution was added to the tube. The tube was then carefully inverted for about 10 times and then kept on ice for 5 minutes. After which, 150 µL of alkaline lysis solution II was added to the tube. The tubes were gently inverted again for mixing and kept on ice for 5 minutes. It was then centrifuged at 10,000 rpm for 5 minutes at 4°C. Transfer the supernatant to fresh microfuge tubes and add an equal volume of tris saturated phenol and chloroform isoamyl alcohol. Mix well and then centrifuged at 10,000 rpm for 5 minutes at 4° C. Transfer the aqueous phase to fresh tube. Add an equal volume of chloroform isoamyl alcohol. Mix well and centrifuge at 10,000 rpm for 5 minutes at 4° C. The top layer was collected and 1 volume of ice cold isopropanol was added and kept on ice for 30 minutes. The mix was centrifuged at 10000 rpm for 5 minutes at 4 ° C. Pellet was washed with 1 volume of 70% ethanol and centrifuged at 10000 rpm for 5 minutes at 4°C. The pellet was dried until the ethanol evaporated. The pellet was then dissolved in 20 µL sterile distilled water and vortexed at 37°C for 15 minutes. The presence of the plasmid was confirmed by running a 0.7 % agarose gel at 70 V for 1 hour.

3.4.5 Transfection of HEK 293 cells and PC 12 cells with pEGFP-C1

Transfection of the cells were carried out by two methods- Calcium phosphate mediated transfection and with the aid of X-Treme GENE HP DNA Transfection reagent

3.4.5.1 Calcium phosphate mediated transfection

Calcium phosphate mediated transfection was carried out as described by D.W Russel, 2011.

Day 1

Seeding of cells- Approximately 10^5 cells /mL was seeded on a 35 mm cell culture dish. Two dishes were seeded. Dish 1 acted as a control and Dish 2 as control.

Day 2

One hour before the transfection, media was changed in the wells.

Preparation of Calcium phosphate-DNA mix

25 µg of pEGFP-C1 was added to a tube containing 100 µL of 2.5 M Calcium chloride. It was made upto 1 mL with 0.1 X TE Buffer (pH 7.6). The mix was incubated for a few minutes. 200µL of HEPES Buffered Saline was added, incubated for 5-10 minutes and 200 µL of this mixture was added over the cells. To the control dish, 200µL of Calcium chloride- HEPES was added (without the plasmid). The dishes were then incubated for 5-6 hours and the media containing the precipitate was aspirated off and fresh DMEM added. The dishes were then incubated in the CO_2 incubator overnight. The fluorescence is measured after 24-48 hours (Sambrook and Russell 2001).

3.4.5.2 X-Treme GENE HP DNA Transfection reagent

HEK-293 cells were transfected with pEGFP-C1 by using X-Treme GENE HP DNA Transfection reagent, Roche as per the product protocol recommended by the manufacturer.

pEGFP-C1 approximately 1.2 µg/µL was dissolved in sterile water . The concentration and purity (260/280 ratio) of pEGFP-C1 was determined by using ND-1000, Nanodrop spectrophotometer. The desirable concentration and purity being 0.1-2 µg/µL ; 260/280 ratio being 1.8.

Day 1

24 hours before transfection , optimal concentration of cells(3.7×10^4) were plated into the desirable number of wells in a 24 well plate.

Day 2

The X-Treme GENE HP DNA Transfection reagent, DNA and diluents were brought to room temperature. Then, the glass vial containing the reagent was vortexed. 100µL of diluents containing 1µg DNA was added to a 1.5 mL microfuge tube. 2 µL of the reagent was pipette directly into the medium containg the diluted DNA without coming into contact with the walls of the tube. The transfection reagent: DNA complex is then incubated for 15 minutes at 15°C. Then, the transfection complex was added to the cells in a dropwise manner. The cells were then incubated for 18-72 hours and then the fluorescence was observed using a fluorescent microscope.

Results and Discussion

CHAPTER 4

RESULTS AND DISCUSSION

4.1 Scaffold Synthesis and Stabilization

The copper capillary alginate scaffold was fabricated with ease and then further on stabilized by cross linking with Hexamethylene di isocyanate. This stabilized the scaffold and to remove the free copper ions the scaffold was washed successively with HCl. This removed the copper ions and changed the pale blue colour of the scaffold which is basically due to the entrapment of copper ions. To promote the attachment of the cells on the scaffold , it was coated with chitosan. It was observed that crosslinking and chitosan coating did not change the properties of the scaffold much other than rendering it more stable.

The following sections describe characterization of the scaffolds and their ability to allow cell attachment and growth.

4.2 Scaffold Characterization

The scaffolds were analyzed for its structural properties using optical microscopy (OM) and environmental scanning electron microscopy (ESEM) and degradation studies reported here provide a solid foundation for future work. Optical microscopy studies essentially report on copper capillary alginate scaffold morphology. The SEM studies describe the morphology and composition (with the help of energy dispersive spectroscopy, EDS). The degradation study could help in elucidating the scaffold's water content resulting from different stabilizing methods.

4.2.1 Optical Microscopy

The IX 51 light microscope from Olympus (Japan) equipped with Rolera-XR Mono Fast 1394 Video Camera from Q Imaging provided an effective and digital capture microscope system. The images captured with this setup were used for obtaining quantitative measurements and surface topography of the scaffolds.

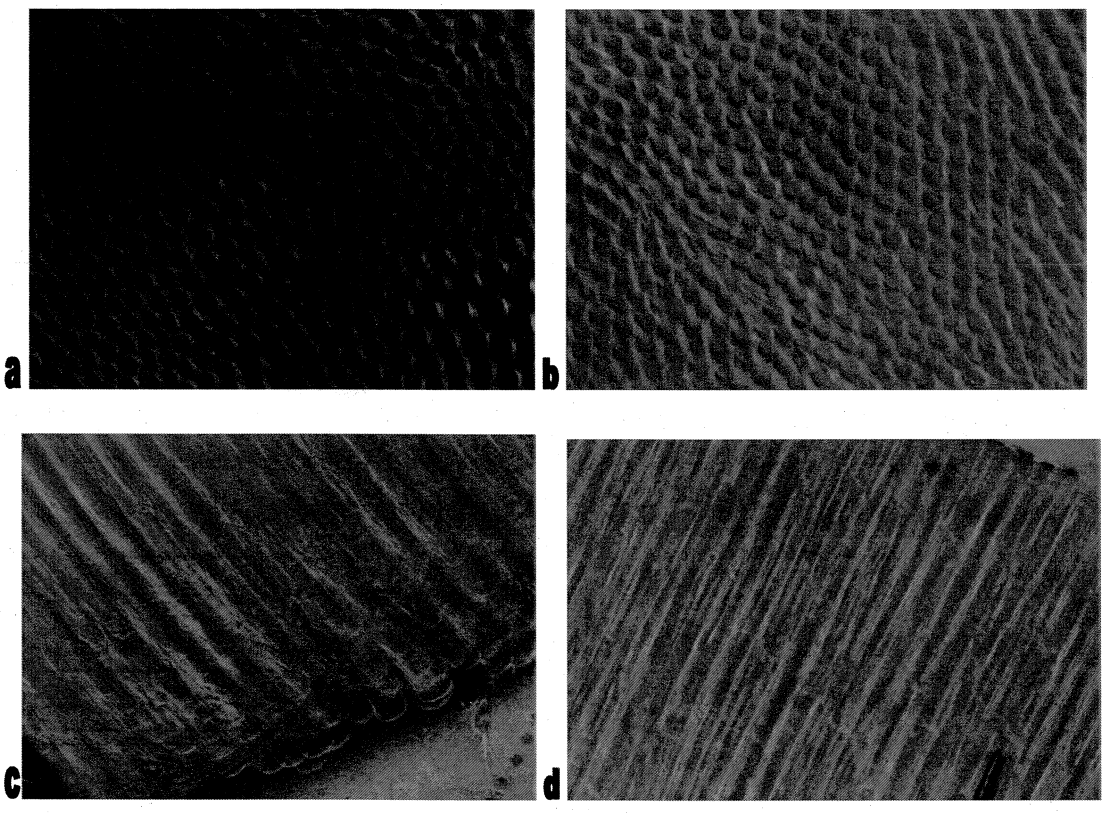

Figure 14. Optical Microscopic images of CCAG. Cross sectional view of raw CCAG Scaffold (a) and Chitosan coated cross linked CCAG (b)(4 X magnification); Transverse section of CCAG Scaffold (c) Chitosan coated cross linked CCAG (d)(10 X magnification). The results show that there are no significant differences in capillary diameters and arrangement of capillaries following cross-linking and coating with chitosan.

4.2.2 Copper capillary alginate scaffold

The capillaries in copper aliginate scaffolds showed an uniform distribution with a diameter ranging from 16μm to 80μm (Figure 14 a-d). The average capillary diameter of the upper, lower and middle regions of the scaffold (Figure 15) suggested that there are variations in diameter as the capillaries develop deeper into the scaffold region. Besides, the parallel nature of capillaries were highly reproducible (Figure 14 c, d) in each batch synthesized. It was found that the average capillary diameters varied significantly from each other for all the samples from different batches. This maybe either due to the fact that the cross linking ion within a given gel are not consistent or there is significant error that is involved in the sample sectioning, the latter being the most suspected case. The major difficulty in sectioning was removing the upper region of the gel, which had varying thickness among the batches. This variation had significant effect on the diameter of the capillaries. Options like keeping the copper solution levels and alginate in a constant level did not helped in formation of predictable capillaries with same diameter. Since the capillaries showed a tapering effect as the depth increases, we decided to take the middle most sections of the scaffolds with an average diameter of approximately 33 μm which had more capillaries of uniform, dimensions.

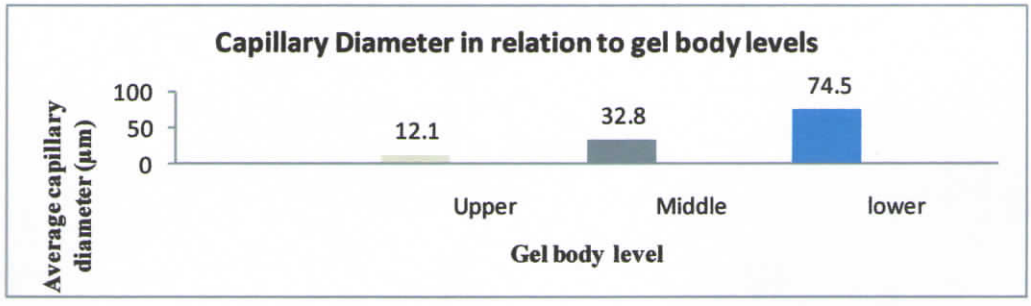

Figure 15. Graph showing capillary diameter in relation to the gel body levels. The Upper gel sections showed thinner capillaries with an average diameter of (12.1μm), the middle section showed uniform distributions of pores with a uniform diameter of 61.7μm and the lower section showed an average pore diameter of 92.3 μm.

4.2.3 Degradation and Hydrolysis

The copper capillary alginate scaffold showed structural degradation once placed in PBS or water (Figure 16). the leaching out of copper ions was immediate when placed in PBS. The complete structure was lost after a period of 48 hours. However, when kept in deionized water the scaffold did not degrade out. Degradation of the scaffold could be due to the exchange of copper ions with the free ions in the water.

4.2.4 Cross linking the CCAG with HDI and coating with chitosan

Because of the degradation of the copper capillary alginate in water , it was then cross linked with Hexamethylene Diisocyanate (HDI). The cross linked copper capillary alginate scaffold was further on coated with chitosan after cross linking with HDI to enhance the attachment of cells on it. The capillary dimensions were not affected by the coating (Figure 14 b and d). The CCAG scaffold following cross linking showed more stability, however degradation did happen following incubation after 5 days in PBS.

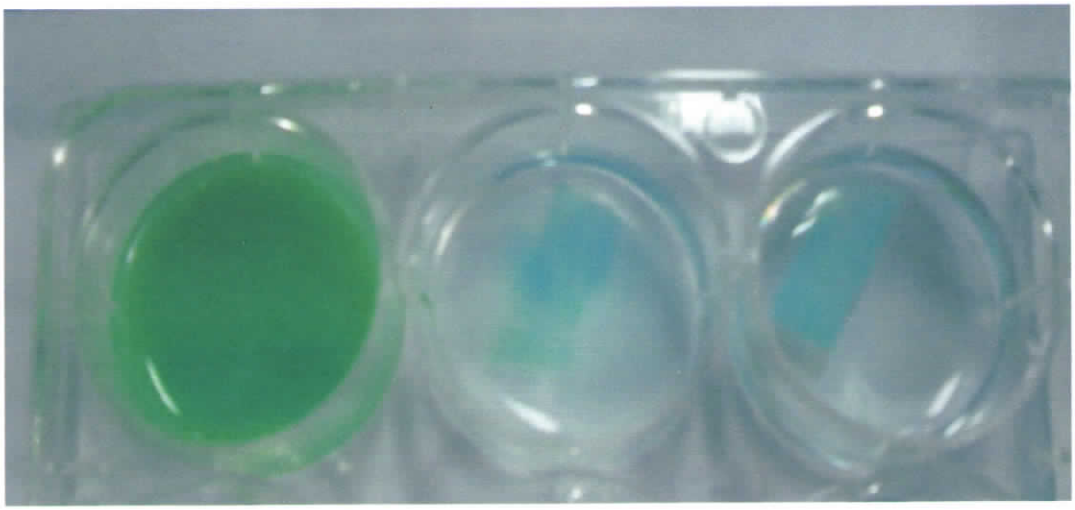

Figure 16 Scaffold degradation studies. Figure 4 Scaffold degradation a) Well 1 shows CCAG in PBS b) Well 2 shows raw CCAG scaffold in sterile water c) Well 3 shows crosslinked CCAG in PBS. The CCAG degraded when placed in PBS and sterile water (within few minutes). Meanwhile the crosslinked CCAG remained stable when placed in PBS (5 days).

4.2.4 Scanning Electron Microscopy/Energy Dispersive Spectroscopy (SEM/EDS)

a)

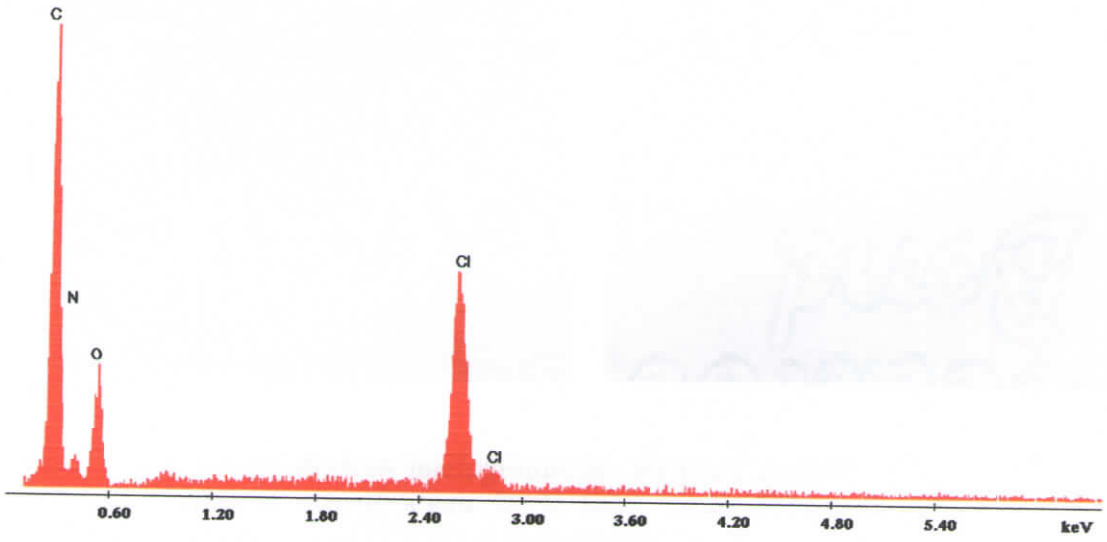

b)

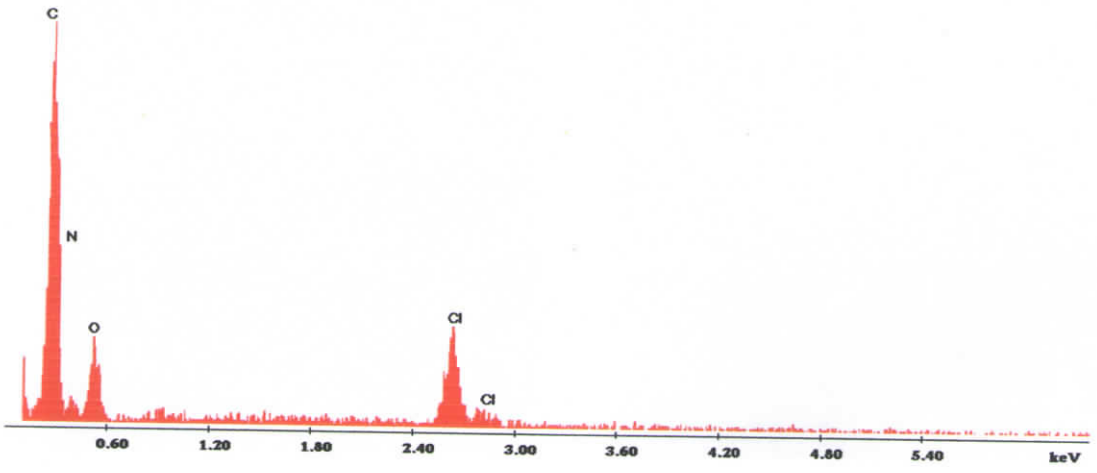

Figure 17 SEM-EDS Elemental analysis (a) EDS Spectrum of CCAG after HCl washing for proton exchange (b) EDS Spectrum of CCAG after subsequent washes with water to remove chlorine. The EDS data reveals that the copper ions have been removed following proton exchange. The chlorine peak maybe due to successive HCl washes. Chlorine peaks have reduced following washing procedure.

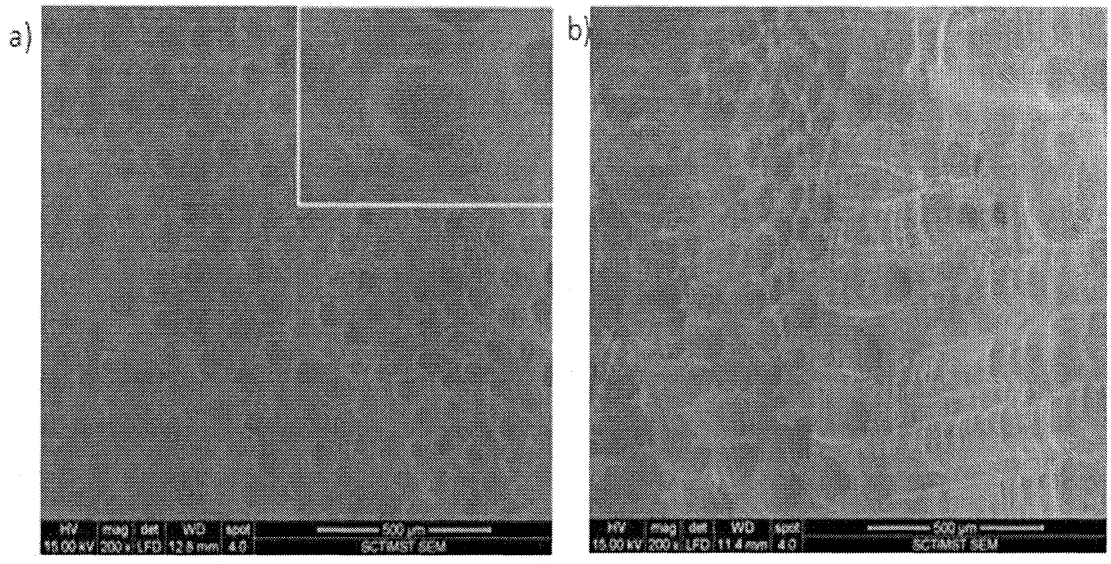

Figure 18. Scanning electron micrographs of RCCAG scaffold. (a) Cross section view of RCCAG at magnifications 200X (inset image 1500X magnification) (b) Longitudinal section view of RCCAG at magnification 200 X

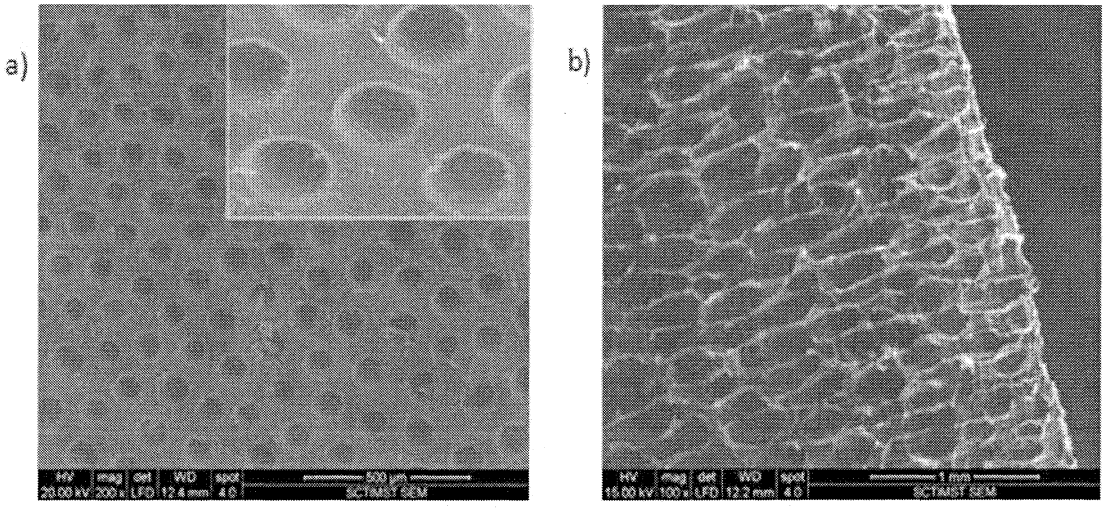

Figure 19. Scanning electron micrographs of CCAG after cross linking with HDI (a) Cross section view of CCAG at magnifications 200X(inset image 1500X magnification) (b) Longitudinal section view of CCAG at magnification 100X. SEM images also suggests that there are no significant changes in capillary dimensions or morphology following crosslinking with Hexamethylene diisocyanate

The copper capillary alginate scaffolds after cross linking and proton exchange were analyzed for the trace elements present. EDS analysis shows that the cross linked scaffold chiefly consists of carbon, oxygen and nitrogen (Figure 17). The carbon, nitrogen and oxygen are the sole components of the alginate polymer. Traces of copper from copper nitrate were expected but did not show up in the EDS analysis data. Chlorine peaks were also observed. Chlorine could presumably be left on the scaffold due to the HCl washes for removing the copper ions from the scaffold. A second EDS was done to determine if the chlorine levels decreased following a few exchanges with water (Figure 17. b) but did not show much variation though the peak profile showed attenuation of chlorine level. However, in EDS analysis caution should be exercised when attempting to assess the quantitative values of the elements present. The peaks of elements that are actually present in high concentrations (particularly elements with smaller atomic number) can appear as smaller than peaks of elements present in small concentrations. The correction matrix is complicated and the variables used are usually poorly known for low atomic number elements leading to semi-quantitative data at best. Scanning electron micrographs of the copper capillary alginate scaffold after cross linking showed that the scaffold has a smooth surface with pentagonal and hexagonal shaped parallel capillaries (Figure 18 and 19). The capillary diameters within the diameter range of 30 μm to 60μm. (Figure 19)

4.2.5 Micro-CT Imaging

The scaffolds were scanned using a cone-beam high-resolution micro-CT 40. Approximately 300 slices were acquired. Data sets were reconstructed using standardized cone-beam algorithm based reconstruction software, ScanCo Medical analysis. A standardized threshold value of 60 to 1000 grey level was applied. Anisotropic channels were observed in the two dimensional slices. Three dimesnsional morphology of the scaffold could be observed. (Figure 20) These images reveal that in some areas the channels are discontinuous but are parallel. But at some areas these channels are discontinuous.(Figure 21) A comparison in the pore size distribution of scaffolds made with 1 % alginate and 2% alginate was done. Micro CT data revealed that in the CCAG

scaffolds made with 1 % alginate had greater pore diameters when compared to the scaffolds made with 2% alginate (Figure 23 a and b). Approximately, 42% of the capillaries have a pore diameter of 64 μm in 1% alginate (Figure 23. a). The scaffolds made with 2% alginate approximately 39% of the pores have a pore diameter of 32μm (Figure 23 b). The data suggested that as the percentage of alginate increases, there is a shift towards forming larger capillaries (see Figure 23). In 1% alginate solution, majority capillaries were falling below 64um with a highest pore size of 112μm. In 2% alginate there is a significant shift towards higher size capillaries above 32um to a maximum size of 144μm. Hence it is essential to standardize the alginate percentage to adjust the level capillary diameter within the scaffold. The wall thickness analysis showed that the capillary formation has significant correlation with the percentage of alginate. 1% alginate has a larger wall thickness of 14μm compared to 2% alginate of 4um; (Figure 21, 24 a and b), suggesting a higher density of capillary formation as the percentage of alginate increases.

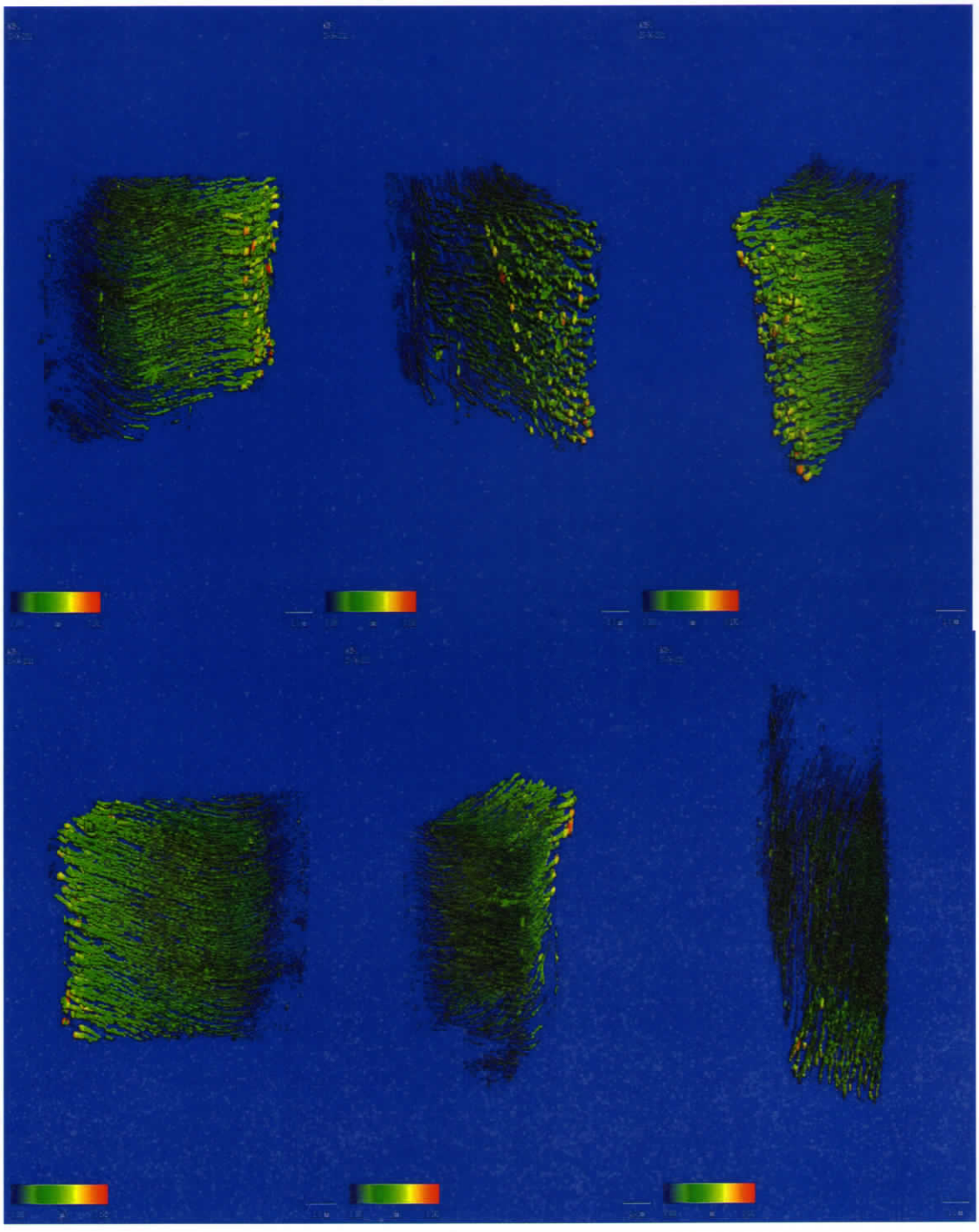

Figure 20. Pore size distribution within the CCAG determined using Micro CT. Shows that the pores distributed more or less uniformly and are mostly of the same pore diameter

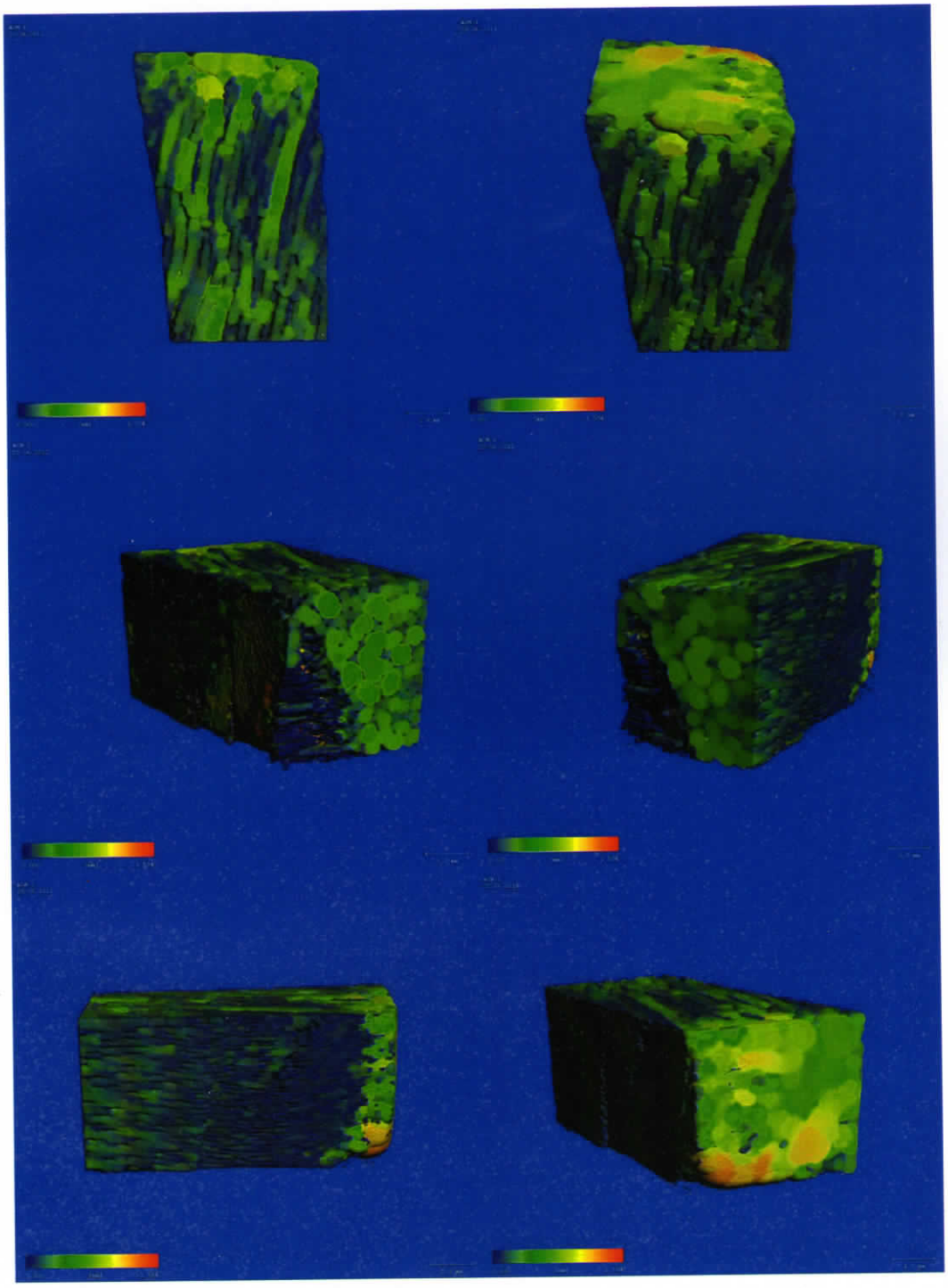

Figure 21. Wall thickness distribution estimated with Micro CT

4.3.2 Transfection studies

4.3.2.1 HEK-293 Cells

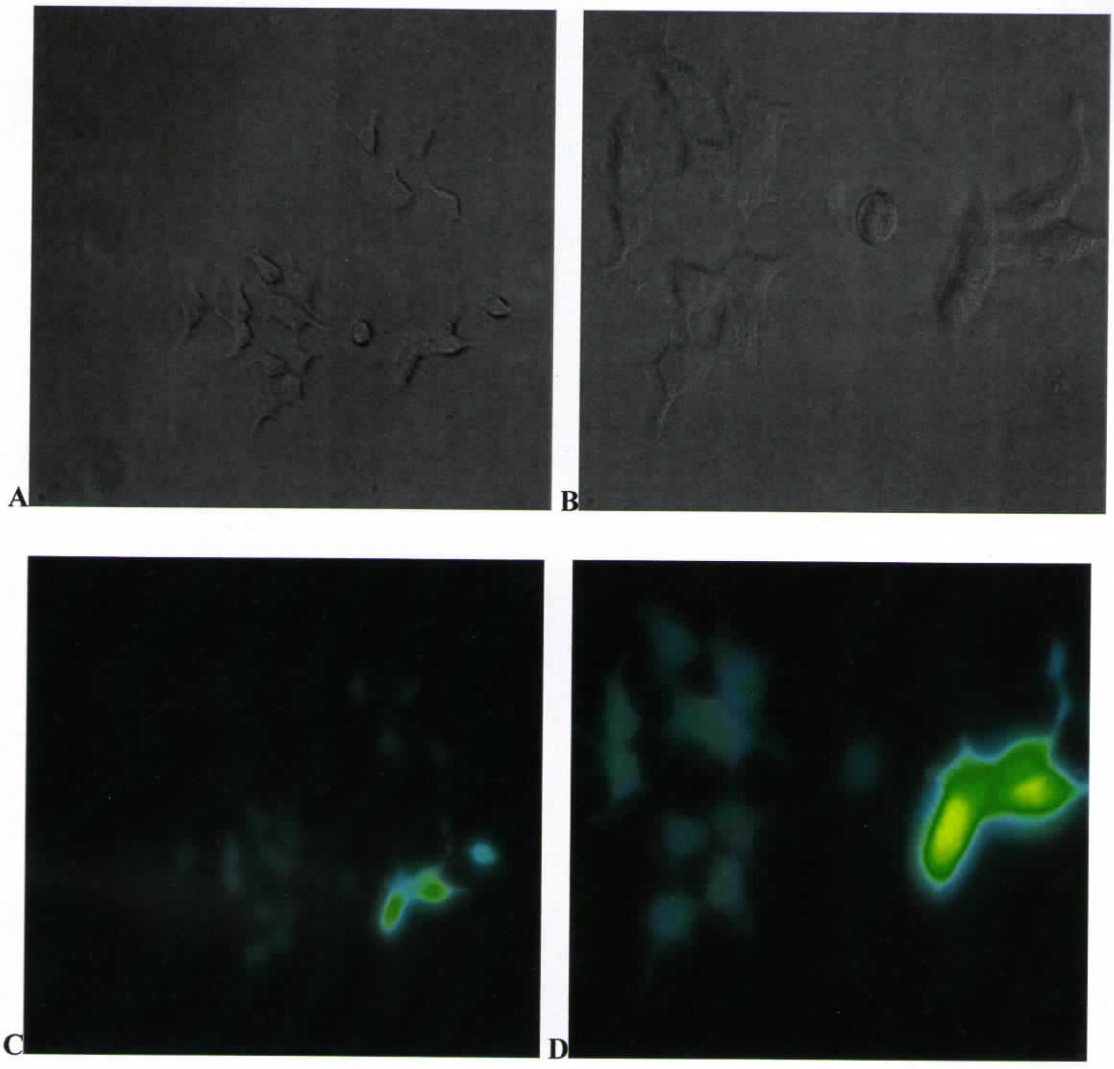

Figure 25: Transfection of HEK 293 cells with pEGFP-C1 . A and C: cells under white light; C and D : cells expressing GFP (under UV 460-580nm) . Transfection of HEK 293 cells with EGFP was carried out successfully by both calcium phosphate and the X-TREME GENE HP DNA transfection kit. Fluorescence was observed following incubation for 48 hours. (magnification A and C 20X; C and D 40X).

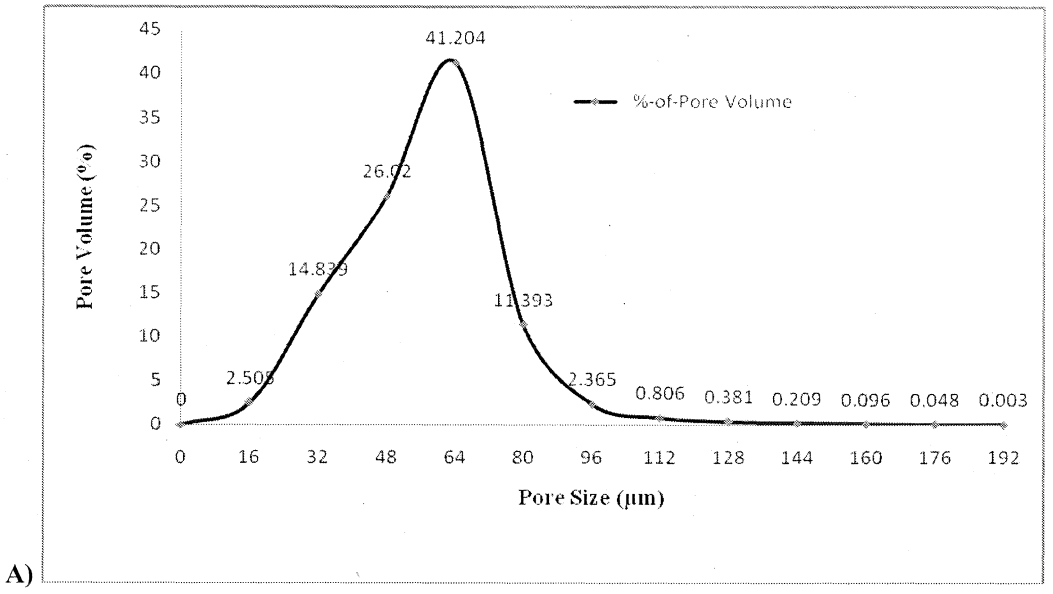

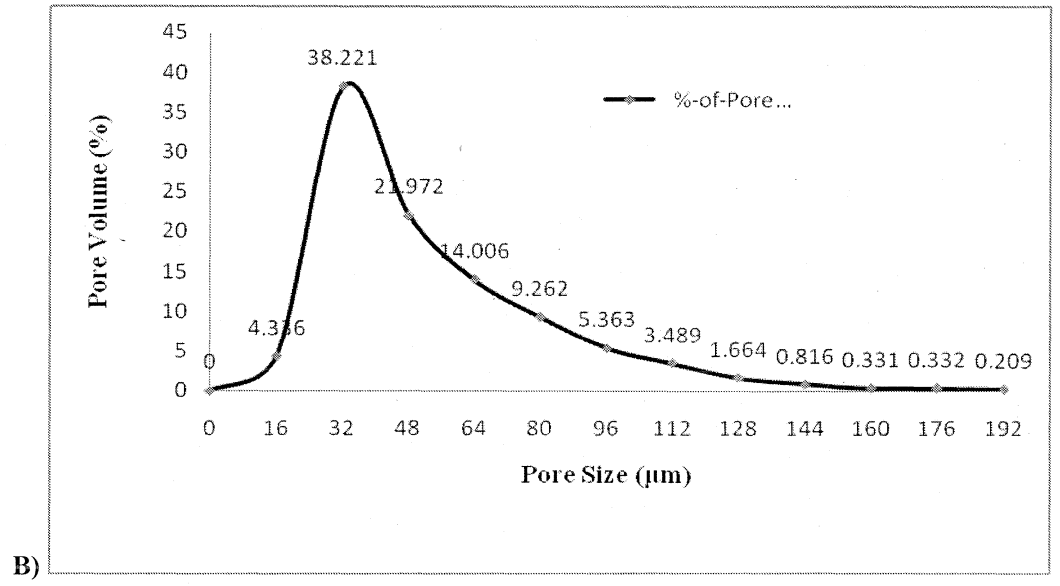

Figure 22. : Pore size distribution within the CCAG. A) 1% alginate CCAG B) 2% alginate CCAG.The data shows that 42% of the capillaries have a pore diameter of 64 µm in 1% alginate and 39% of the pores have a pore diameter of 32µm. In 1% alginate solution, majority of the capillaries fall below 64um with a highest pore size of 112µm. In 2% alginate there is a significant shift towards higher size capillaries above 32um to a maximum size of 144µm.

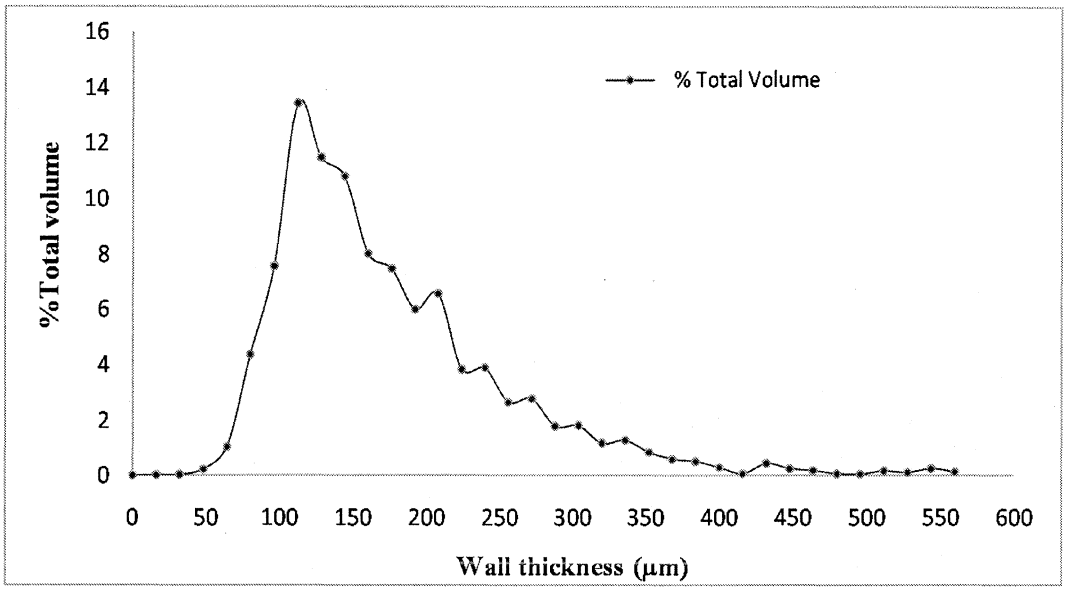

A)

B)

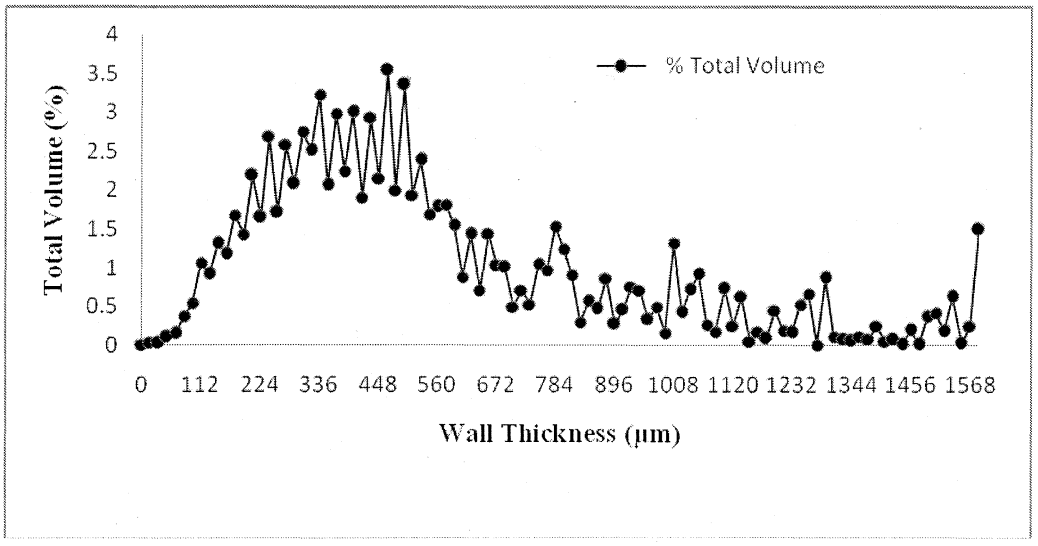

Figure 23.: Wall thickness distribution within the CCAG 1% alginate CCAG B) 2% alginate CCAG The wall thickness analysis shows that capillary formation has significant correlation with the percentage of alginate used. 1% alginate has a larger wall thickness of 14µm compared to 2% alginate of 4µm implying that the capillaries would be more closer together in CCAG with higher percentage of alginate

4.3 Biological assessment of the scaffold

The main point of the biological experiments discussed below was to assess 1) if cells could be seeded in and on the newly developed scaffolds and 2) if these seeded cells could survive and proliferate over the course of several days.

4.3.1 Cell culture studies

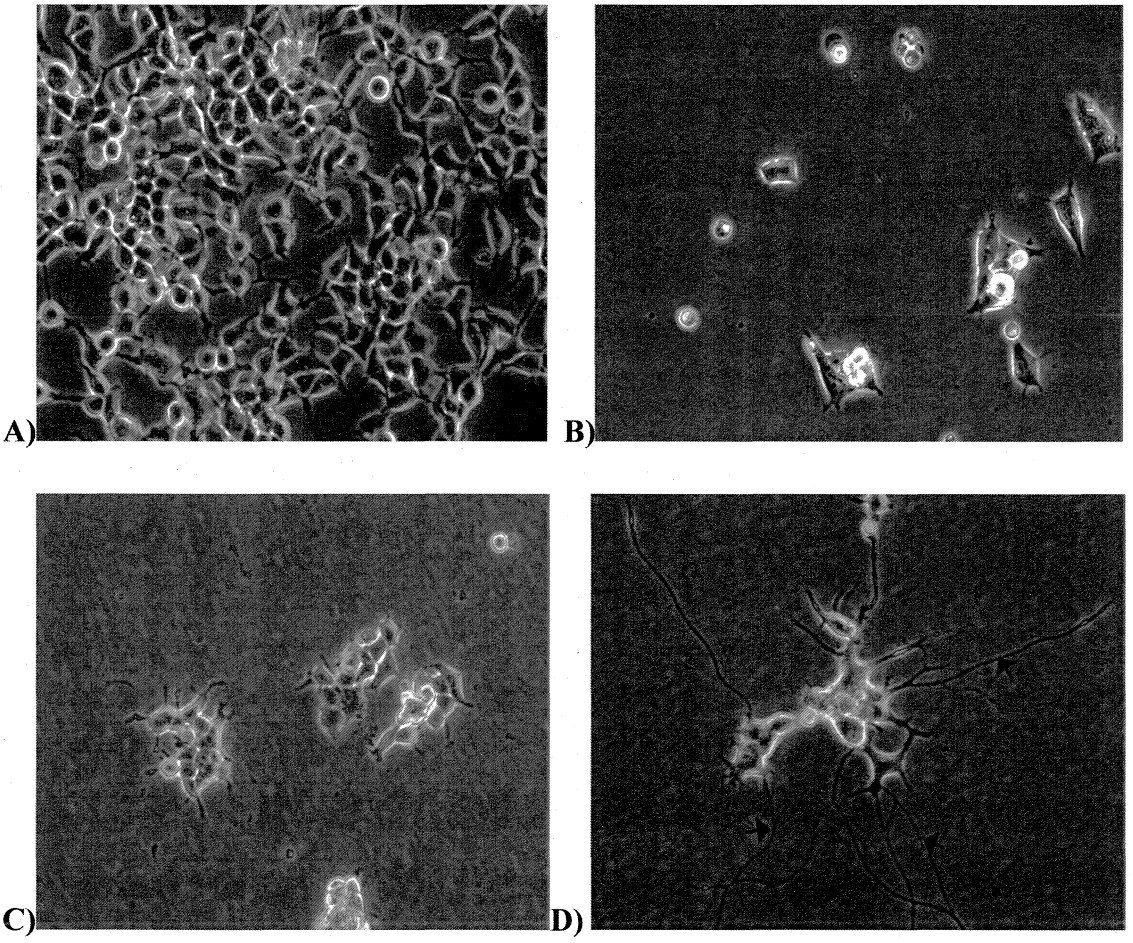

Figure 24. Standardization of culture of HEK 293 and PC 12 A) HEK 293 cells on 3rd day in culture (Magnification, 20X) and B) HEK 293 cells (Magnification, 40X) PC 12 cells prior to NGF treatment (20X) D) PC 12 cells (after NGF treatment); Magnification 20X. HEK-293 cells and PC -12 cells were successfully maintained and optimized for further studies. PC-12 responded to Nerve Growth factor and extended neurites in its presence (arrow heads in figure D).

4.3.2 Transfection studies

4.3.2.1 HEK-293 Cells

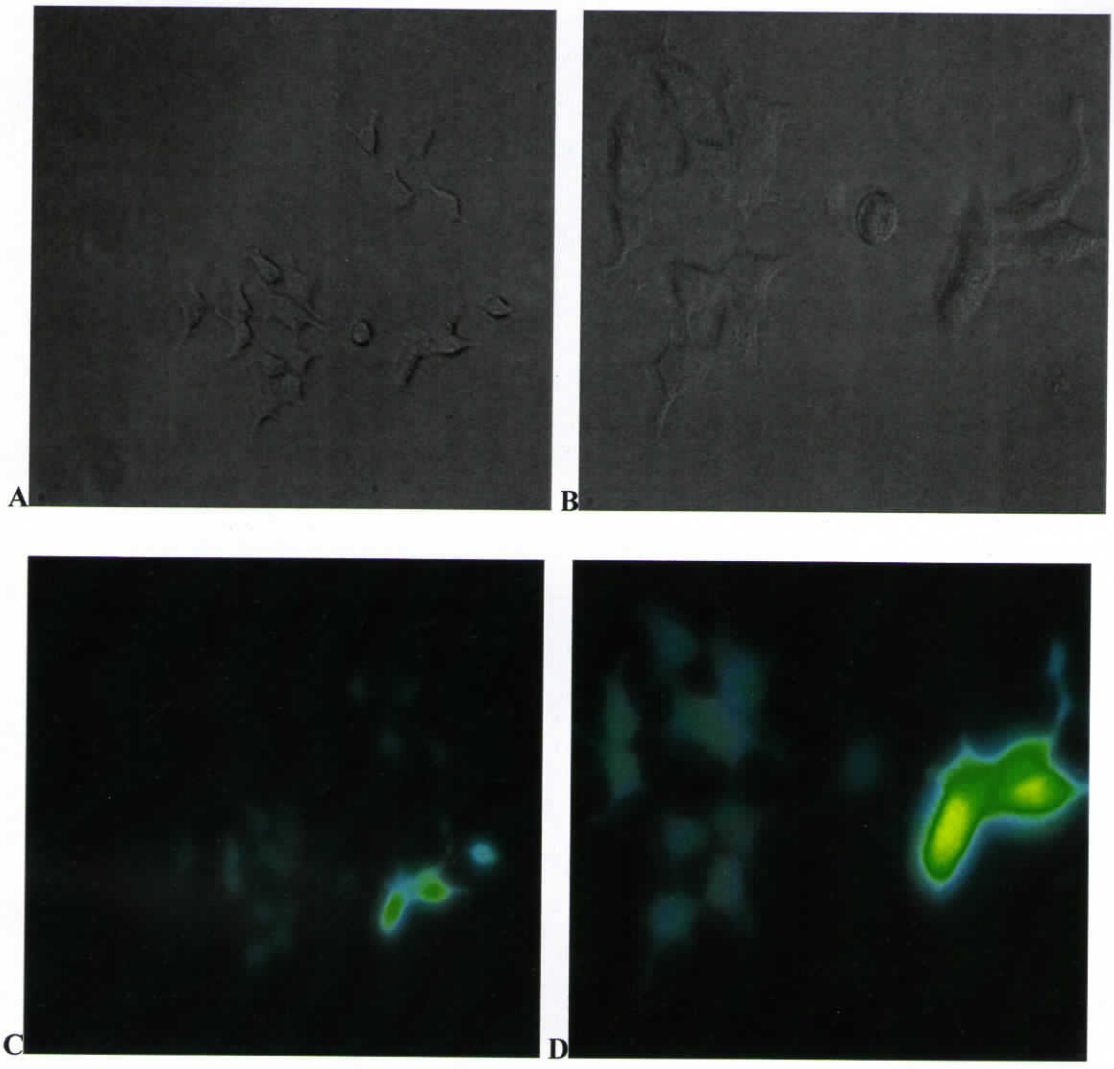

Figure 25: Transfection of HEK 293 cells with pEGFP-C1 . A and C: cells under white light; C and D : cells expressing GFP (under UV 460-580nm) . Transfection of HEK 293 cells with EGFP was carried out successfully by both calcium phosphate and the X-TREME GENE HP DNA transfection kit. Fluorescence was observed following incubation for 48 hours. (magnification A and C 20X; C and D 40X).

4.3.2.2 PC 12 cells

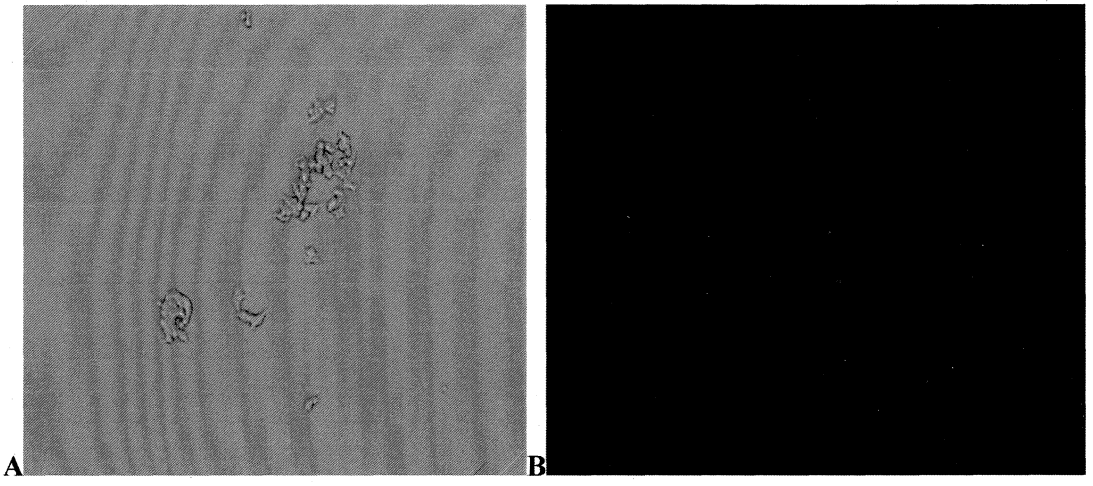

Figure 27: Transfection of PC 12 cells with pEGFP-C1 Figure 27: Transfection of PC 12 cells with pEGFP-C1 A) under white light and B)under under UV (480-560nm). The cells failed to uptake the plasmid under the experimental conditions. (Magnification 10X).PC 12 cells have been found to be resistant to transfection by calcium phosphate method probably due to the small size and low cytoplasmic content.

Tranfection of HEK 293 cells was carried out by both Calcium phosphate method (Sambrook and Russell 2001) and with X-Treme GENE HP DNA Transfection reagent. Fluorescent signals were observed following incubation for 24-48 hours (Figure 4.10). Attempts to transfect PC 12 cells with the Calcium phosphate method and the X-Treme GENE HP DNA Transfection reagent met with very little success. PC12 cells are known for its resistance to transfection with calcium phosphate method. Its recommended to use Amaxa based electro-transfection system for transfection (Nucleofector ™) in these types cells.

4.3.3 Seeding cells on the CCAG scaffold

The primary aim of cell culture studies was to determine if the cells could be seeded on the synthesized CCAG scaffold. The CCAG scaffold was sterilized by treating with 70% ethanol. PC 12 cells were then seeded on the scaffold.

A) 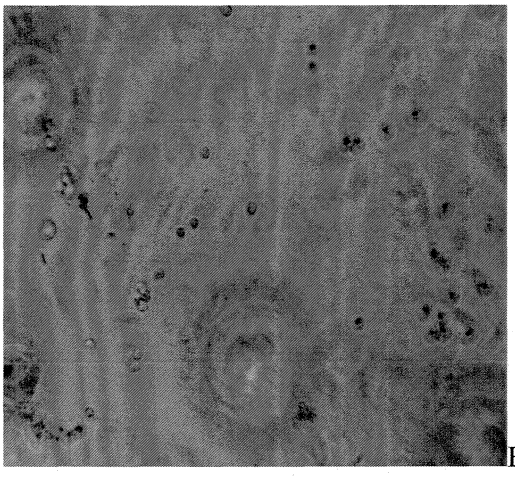 B) 

C) 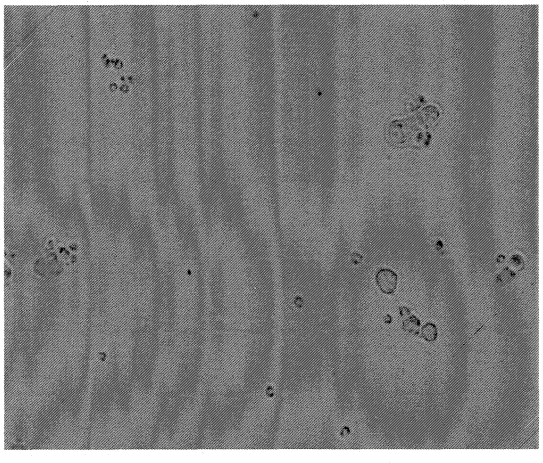

Figure 28: Seeding of PC 12 cells on CCAG A) PC 12 cells on CCAG (10 X magnification) B) PC 12 cells on CCAG (20X Magnification) C)PC 12 Cells seeded on well area without scaffold (20X magnification). However attachment of the cells to the scaffold was very low when compared to the attachment of the cells in the well without any scaffold

PC 12 cells were seeded on the CCAG scaffold . However, there was only limited attachment of the cells to the scaffold (Figure 4.16).

4.3. Live dead staining

The viability of the cells on the scaffold was determined using a live dead assay, the live cells were stained with Calcein AM and the dead cells were stained with Ethidium bromide.

A) 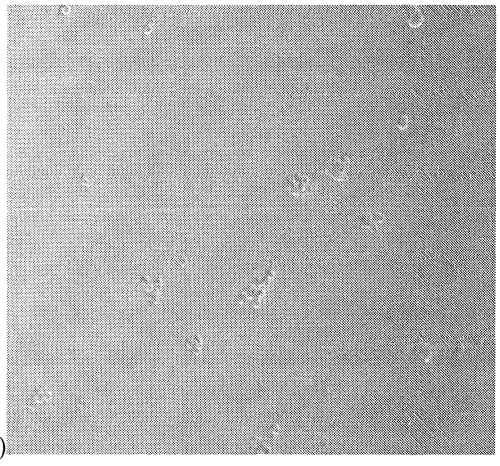 B) 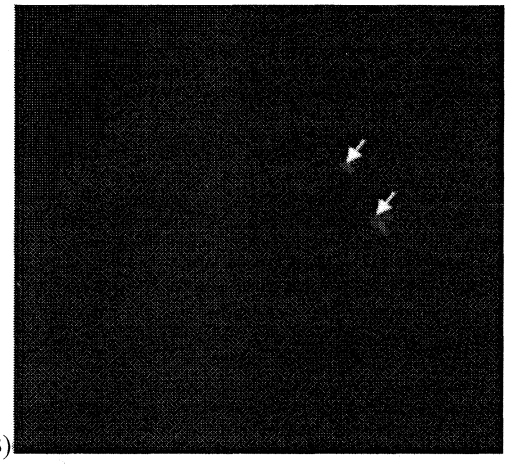

Figure 29: Live dead staining. Dead cells stained with EtBr A) Captured at 10 X B) Captured at 40 X. Live dead assay was carried out by adding the scaffold extract to a well plated with the HEK 293 cells and then staining with ethidium bromide. The staining revealed that few cells undergoing apoptosis.(See arrowheads)

Initially, a lot of cell death was observed probably due to the inhibitory action of the crosslinker (hexamethylene di isocyanate) or the free copper ions and chlorine residue. The cell mortality was estimated and was found to be approximately 28%.

Eventhough the scaffold was synthesized successfully, there were several technical issues to be dealt with during this procedure. The copper alginate scaffold synthesized by the spray method did not show continuity in formation of channels. The alginate coated petri dish was a much better alternative to the spray method. After synthesis, the copper

capillary alginate scaffold was not stable when placed in cell culture media or for that matter in PBS. Within the course of several hours (< 24 hours) in Dulbecco's Minimum Esssential Medium (DMEM) , the scaffold started to disintegrate. This may be due to either the chelation of copper ions or exchange of Cu^{2+} with the ions present in the medium. Therefore a method had to be devised to strengthen or stabilize the scaffold without losing the inherent channels formed within the Copper capillary alginate scaffold. Attempts were made to stabilize the scaffold by coating the scaffold with chitosan which did not yield the desired results. The scaffold was then successfully crosslinked by means of using a chemical crosslinker, hexamethylene diisocyanate. Though the scaffold synthesis as such was quite straightforward, the stabilization part seemed to be tricky. As mentioned in previous literature, the coating of the petri dish with a thin layer of alginate seemed to be necessary and the use of tissue paper to aid in the formation of a uniform and regular primary membrane made the descending capillary formation much easier and uniform when compared to the spray method. The scaffold synthesized in this manner has copper ions within it, and is pale blue in colour. This makes it less attractive for application in vitro testing conditions. When compared to the alginate scaffold produced by chelation with calcium ions, the copper capillary alginate scaffold was more durable. Cutting the scaffold proved to be more difficult in the direction parallel to the capillary axis than cutting it perpendicular to the long axis. The anisotropic nature of the scaffold is primarily due to the fact that alginate chains are preferentially oriented perpendicular to the long axis.

Chitosan coating of the CCAG was successful. However, there were no significant changes in the pore dimensions and structure of capillaries following coating. Washing the scaffold with media caused changes in the scaffold. All of the copper present in the scaffolds as free ions or otherwise appears to be removed with successive washing. Free copper ions are leached out or chelated serving to decolorize the scaffold. This resulted in a translucent scaffold with a completely distorted morphology. The channels and pores in

the scaffold were no longer visible. Hence crosslinking the scaffold with hexamethylene di isocyanate and then coating it with chitosan seemed to be the best methodology.

Copper capillary alginate scaffold could be successfully synthesized and stabilized. However, certain modifications with regard to enhancing the attachment of cells such as coating with extracellular matices and providing chemical guidance cues could help in overcoming the shortcomings of the scaffold as such. The parallel channels within the CCAG could be potentially utilized for understanding the mechanism of axonal pathfinding and guidance.

Summary and Conclusion

Chapter 5

Summary and Conclusion

Hydrogels like alginate and agarose have many favorable properties which make them very useful for various applications. They have mechanical and physicochemical properties that resemble the host tissue. Alginate has an interesting ability to form anisotropic linearly oriented channels within them. The central aim of this study was to determine if such an alginate scaffold with linearly arranged channels could be created and if so whether it could help in axonal elongation. The CCAG scaffolds were fabricated successfully. It was found that the diameter of these channels can be varied depending on the application by changing the alginate and electrolyte concentration. It was found that the channels could be created by superimposing with a copper nitrate solution and that these channels were parallel. It was hypothesized that these channels could promote axonal regeneration in an organized manner. The channels in the scaffolds fabricated were not continuous in certain locations. By varying the alginate concentration the dimensions of the pore dimensions of the capillaries could be varied. The diameters of the capillaries in the scaffold fabricated varied between 16 μm and 80μm with 2% alginate CCAG and 16 μm to 112 μm with 1% alginate CCAG. The scaffold was characterized to understand its properties. Optical microscopy and Scanning electron microscopy provided conclusive results about the pore dimensions and morphology of the channels. Degradation rates were studied to understand the stability of the scaffold. Micro CT was done in order to understand the exact three dimensional structure of the scaffold and to know the pore distribution and wall thickness. Cell culture studies were conducted but did not reveal much conclusive data. Transfection of HEK-293 cells was standardized successfully. However, PC 12 cells could not be successfully transfected. PC 12 cells were seeded on to the scaffold to understand the biocompatibility of the constructed scaffold. Live dead staining was carried out to understand the viability of the cells on the scaffold. Mortality rates were high initially but washing the scaffold with many changes of water could reduce the problem. Mortality rates were estimated to be equivalent to be approximately equal to 28%. More *in vitro* studies have to be conducted to

standardize transfection of PC 12 cells for studying the dynamics of neurite extension within the scaffold. Also, it would be helpful to know whether significant changes in capillary dimensions could affect the axonal extension and pathfinding. It is presumable that this capillary alginate system could be helpful to test axonal regeneration *in vitro* and significant modifications to the scaffold in terms of adhesion molecules, neurotrophic factor release, different cell types etc., could help in understanding the exact mechanism of axonal pathfinding. The central aim of this work was to develop capillary alginate scaffolds. Many of the studies are just early stage and much more experiments have to be conducted to understand the full potential of these scaffolds.

Future prospects

More scaffolds with various parameters such as different divalent ions instead for copper, different types and concentrations of alginate have to be formulated to fully understand these scaffolds. Synthesizing the raw copper capillary alginate scaffold is a fairly easy task when compared to the modifications to be done to make the CCAG to be applicable for its intended use. The characterization of scaffold did provide a lot of information as to the exact properties of the scaffold. Even though EDS in itself is a powerful quantitiative elemental analysis tool, the results obtained were not very conclusive. A more suitable method of analysis such as mass spectrometry could reveal more conclusive quantitative elemental analysis data. The priority should be to understand the presence of the copper ions and residues of chlorine and HDI. Fourier transform infrared spectroscopy (FTIR) studies could also help in obtaining conclusive quantitative surface composition data. In terms of biological studies, more experiments need to be done. A more appropriate method of seeding the cells on the scaffold has to be developed. Also, fluorescent labeled cells could help in tracing the exact mode of migration and neurite extension within the scaffold. Furthermore, the effect of various extracellular matrices and diffusible neurotrophic factor release should also be attempted with the scaffold.

Bibliography

References

Amado, S., M. J. Simões, et al. Use of hybrid chitosan membranes and N1E-115 cells for promoting nerve regeneration in an axonotmesis rat model. Biomaterials 2008.**29**(33): 4409-4419.

An, Y., K. K. Tsang, et al. Potential of stem cell based therapy and tissue engineering in the regeneration of the central nervous system. Biomedical materials (Bristol, England) 2006.**1**(2): R38-44.

Auger, F. A., M. Rouabhia, et al. Tissue-engineered human skin substitutes developed from collagen-populated hydrated gels: clinical and fundamental applications. Med Biol Eng Comput 1998.**36**(6): 801-812.

Balgude, A., X. Yu, et al. Agarose gel stiffness determines rate of DRG neurite extension in 3D cultures. Biomaterials 2001.**22**: 1077 - 1084.

Balgude, A. P., X. Yu, et al. Agarose gel stiffness determines rate of DRG neurite extension in 3D cultures. Biomaterials 2001.**22**(10): 1077-1084.

Banker, G. and K. Goslin Culturing nerve cellsCambridge, Mass., MIT Press.1998: xii, 666 p., 611 p. of plates.

Bearer, E. L. An actin-associated protein present in the microtubule organizing center and the growth cones of PC-12 cells. J Neurosci 1992.**12**(3): 750-761.

Bellamkonda, R., J. P. Ranieri, et al. Hydrogel-based three-dimensional matrix for neural cells. J Biomed Mater Res 1995.**29**(5): 663-671.

Bellamkonda, R., J. P. Ranieri, et al. Hydrogel-based three-dimensional matrix for neural cells. Journal of Biomedical Materials Research 1995.**29**(5): 663-671.

Bhatnagar, P., S. S. Mark, et al. Dendrimer-Scaffold-Based Electron-Beam Patterning of Biomolecules. Advanced Materials 2006.**18**(3): 315-319.

Biazar, E., M. Khorasani, et al. Types of neural guides and using nanotechnology for peripheral nerve reconstruction International Journal of Nanomedicine 2010.**5**(1): 839-852.

Boontheekul, T., H.-J. Kong, et al. Controlling alginate gel degradation utilizing partial oxidation and bimodal molecular weight distribution. Biomaterials 2005.**26**(15): 2455-2465.

Bouhadir, K. H., K. Y. Lee, et al. Degradation of Partially Oxidized Alginate and Its Potential Application for Tissue Engineering. Biotechnology Progress 2001.**17**(5): 945-950.

Burdick, J. A., M. Ward, et al. Stimulation of neurite outgrowth by neurotrophins delivered from degradable hydrogels. Biomaterials 2006.**27**(3): 452-459.

Cai, J., X. Peng, et al. Permeable guidance channels containing microfilament scaffolds enhance axon growth and maturation. Journal of Biomedical Materials Research Part A 2005.**75A**(2): 374-386.

Cao, Z., R. J. Gilbert, et al. Simple Agarose−Chitosan Gel Composite System for Enhanced Neuronal Growth in Three Dimensions. Biomacromolecules 2009.**10**(10): 2954-2959.

Cascone, M. G., B. Sim, et al. Blends of synthetic and natural polymers as drug delivery systems for growth hormone. Biomaterials 1995.**16**(7): 569-574.

Chen, R. R. and D. J. Mooney Polymeric Growth Factor Delivery Strategies for Tissue Engineering. Pharmaceutical Research 2003.**20**(8): 1103-1112.

Cui, Z., B. H. Lee, et al. Degradation, cytotoxicity, and biocompatibility of NIPAAm-based thermosensitive, injectable, and bioresorbable polymer hydrogels. Journal of biomedical materials research. Part A 2011.**98**(2): 159-166.

Davenport, R. W., P. Dou, et al. A sensory role for neuronal growth cone filopodia. Nature 1993.**361**(6414): 721-724.

Dent, E. W. and F. B. Gertler Cytoskeletal dynamics and transport in growth cone motility and axon guidance. Neuron 2003.**40**(2): 209-227.

Dichter, M. A., A. S. Tischler, et al. Nerve growth factor-induced increase in electrical excitability and acetylcholine sensitivity of a rat pheochromocytoma cell line. Nature 1977.**268**(5620): 501-504.

Dickson, B. J. Molecular Mechanisms of Axon Guidance. Science 2002.**298**(5600): 1959-1964.

Dillon, G. P., X. Yu, et al. The influence of physical structure and charge on neurite extension in a 3D hydrogel scaffold. J Biomater Sci Polym Ed 1998.**9**(10): 1049-1069.

Drury, J. and D. Mooney Hydrogels for tissue engineering: Scaffolddesign variables and applications. Biomaterials 2003.**24**: 4337 - 4351.

Drury, J. L. and D. J. Mooney Hydrogels for tissue engineering: scaffold design variables and applications. Biomaterials 2003.**24**(24): 4337-4351.

E. Biazar, M. K., N. Montazeri Types of neural guides and using nanotechnology for peripheral nerve reconstruction International Journal of Nanomedicine 2010.**5**(1): 839-852.

Ehrlicher, A., T. Betz, et al. Guiding neuronal growth with light. Proceedings of the National Academy of Sciences 2002.**99**(25): 16024-16028.

Ertürk, A., F. Hellal, et al. Disorganized Microtubules Underlie the Formation of Retraction Bulbs and the Failure of Axonal Regeneration. The Journal of Neuroscience 2007.**27**(34): 9169-9180.

Florian Despang , R. D. a. M. G. Novel Biomaterials with Parallel Aligned Pore Channels by Directed Ionotropic Gelation of Alginate: Mimicking the Anisotropic Structure of Bone Tissue. Advances in biomimetics 2011. 349-372.

Flynn, L., P. Dalton, et al. Fiber templating of poly (2-hydroxyethyl methacrylate) for neural tissue engineering. Biomaterials 2003.**24**: 4265 - 4272.

Foley, J. D., E. W. Grunwald, et al. Cooperative modulation of neuritogenesis by PC12 cells by topography and nerve growth factor. Biomaterials 2005.**26**(17): 3639-3644.

Fournier, E., C. Passirani, et al. Biocompatibility of implantable synthetic polymeric drug carriers: focus on brain biocompatibility. Biomaterials 2003.**24**(19): 3311-3331.

Francis Suh, J. K. and H. W. T. Matthew Application of chitosan-based polysaccharide biomaterials in cartilage tissue engineering: a review. Biomaterials 2000.**21**(24): 2589-2598.

Freed, L. E., G. Vunjak-Novakovic, et al. Biodegradable Polymer Scaffolds for Tissue Engineering. Nat Biotech 1994.**12**(7): 689-693.

Freier, T., R. Montenegro, et al. Chitin-based tubes for tissue engineering in the nervous system. Biomaterials 2005.**26**(22): 4624-4632.

Gadegaard, N., K. Seunarine, et al. 3D fabrication methods for producing tissue engineering scaffolds. Microprocesses and Nanotechnology 2007, Digest of Papers 2007. 410-411
543.

Glowacki, J. and S. Mizuno Collagen scaffolds for tissue engineering. Biopolymers 2008.**89**(5): 338-344.

Gombotz, W. R. and S. Wee Protein release from alginate matrices. Advanced Drug Delivery Reviews 1998.**31**(3): 267-285.

Gomez, N., Y. Lu, et al. Immobilized nerve growth factor and microtopography have distinct effects on polarization versus axon elongation in hippocampal cells in culture. Biomaterials 2007.**28**(2): 271-284.

Greene, L. A. and G. Rein Release, storage and uptake of catecholamines by a clonal cell line of nerve growth factor (NGF) responsive pheo-chromocytoma cells. Brain Res 1977.**129**(2): 247-263.

Greene, L. A. and A. S. Tischler Establishment of a noradrenergic clonal line of rat adrenal pheochromocytoma cells which respond to nerve growth factor. Proc Natl Acad Sci U S A 1976.**73**(7): 2424-2428.

Gunning, P. W., G. E. Landreth, et al. Nerve growth factor-induced differentiation of PC12 cells: evaluation of changes in RNA and DNA metabolism. J Neurosci 1981.**1**(4): 368-379.

Gustavsson, P., F. Johansson, et al. Neurite guidance on protein micropatterns generated by a piezoelectric microdispenser. Biomaterials 2007.**28**(6): 1141-1151.

Isbister, C. M. and T. P. O'Connor Mechanisms of growth cone guidance and motility in the developing grasshopper embryo. Journal of Neurobiology 2000.**44**(2): 271-280.

Jeon, C.-Y., J.-K. Jin, et al. Neurites from PC12 cells are connected to each other by synapse-like structures. Synapse 2010.**64**(10): 765-772.

Kaech, S. and G. Banker Culturing hippocampal neurons. Nat Protoc 2006.**1**(5): 2406-2415.

Kam, L., W. Shain, et al. Axonal outgrowth of hippocampal neurons on micro-scale networks of polylysine-conjugated laminin. Biomaterials 2001.**22**(10): 1049-1054.

Kawase, M., N. Miura, et al. Immobilization of tripeptide growth factor glycyl-L-histidyl-L-lysine on poly(vinylalcohol)-quarternized stilbazole (PVA-SbQ) and its use as a ligand for hepatocyte attachment. Biol Pharm Bull 1999.**22**(9): 999-1001.

Kidane, A., J. M. Szabocsik, et al. Accelerated study on lysozyme deposition on poly(HEMA) contact lenses. Biomaterials 1998.**19**(22): 2051-2055.

Klöck, G., A. Pfeffermann, et al. Biocompatibility of mannuronic acid-rich alginates. Biomaterials 1997.**18**(10): 707-713.

Kobayashi, H., Y. Ikada, et al. Tissue reactions induced by modified poly(vinyl alcohol) hydrogels in rabbit cornea. J Biomed Mater Res 1992.**26**(12): 1583-1598.

Kuo, C. K. and P. X. Ma Ionically crosslinked alginate hydrogels as scaffolds for tissue engineering: Part 1. Structure, gelation rate and mechanical properties. Biomaterials 2001.**22**(6): 511-521.

Langer, R. and J. Vacanti Tissue engineering. Science 1993.**260**(5110): 920-926.

Laurell, T., L. Wallman, et al. Design and development of a silicon microfabricated flow-through dispenser for on-line picolitre sample handling. Journal of Micromechanics and Microengineering 1999.**9**(4): 369-376.

Lee, C. H., A. Singla, et al. Biomedical applications of collagen. Int J Pharm 2001.**221**(1-2): 1-22.

Lee, K., E. A. Silva, et al. Growth factor delivery-based tissue engineering: general approaches and a review of recent developments. Journal of The Royal Society Interface 2011.**8**(55): 153-170.

Lee, K. Y. and D. J. Mooney Hydrogels for Tissue Engineering. Chemical Reviews 2001.**101**(7): 1869-1880.

Lee, K. Y., J. A. Rowley, et al. Controlling Mechanical and Swelling Properties of Alginate Hydrogels Independently by Cross-Linker Type and Cross-Linking Density. Macromolecules 2000.**33**(11): 4291-4294.

Lewis, A. K. and P. C. Bridgman Nerve growth cone lamellipodia contain two populations of actin filaments that differ in organization and polarity. The Journal of Cell Biology 1992.**119**(5): 1219-1243.

Mahoney, M. J., R. R. Chen, et al. The influence of microchannels on neurite growth and architecture. Biomaterials 2005.**26**(7): 771-778.

Mano, J. F., G. A. Silva, et al. Natural origin biodegradable systems in tissue engineering and regenerative medicine: present status and some moving trends. Journal of The Royal Society Interface 2007.**4**(17): 999-1030.

Manz, B., M. Hillgärtner, et al. Cross-linking properties of alginate gels determined by using advanced NMR imaging and Cu 2+ as contrast agent. European Biophysics Journal 2004.**33**(1): 50-58.

Martin, B. C., E. J. Minner, et al. Agarose and methylcellulose hydrogel blends for nerve regeneration applications. J Neural Eng 2008.**5**(2): 221-231.

Meek, M. F. and J. H. Coert Clinical Use of Nerve Conduits in Peripheral-Nerve Repair: Review of the Literature. J reconstr Microsurg 2002.**18**(02): 097,110.

Mueller, B. K. Growth cone guidance: First steps towards a deeper understanding. Annual Review of Neuroscience 1999.**22**: 351-388.

Newman, K. D., C. R. McLaughlin, et al. Bioactive hydrogel-filament scaffolds for nerve repair and regeneration. Int J Artif Organs 2006.**29**(11): 1082-1091.

Nguyen, K. T. and J. L. West Photopolymerizable hydrogels for tissue engineering applications. Biomaterials 2002.**23**(22): 4307-4314.

Norman, J. and T. Desai Methods for Fabrication of Nanoscale Topography for Tissue Engineering Scaffolds. Annals of Biomedical Engineering 2006.**34**(1): 89-101.

Orive, G., S. Ponce, et al. Biocompatibility of microcapsules for cell immobilization elaborated with different type of alginates. Biomaterials 2002.**23**(18): 3825-3831.

Pawar, K., R. Mueller, et al. Increasing capillary diameter and the incorporation of gelatin enhance axon outgrowth in alginate-based anisotropic hydrogels. Acta Biomaterialia 2011.**7**(7): 2826-2834.

Perka, C., R. S. Spitzer, et al. Matrix-mixed culture: new methodology for chondrocyte culture and preparation of cartilage transplants. J Biomed Mater Res 2000.**49**(3): 305-311.

Prang, P., R. Müller, et al. The promotion of oriented axonal regrowth in the injured spinal cord by alginate-based anisotropic capillary hydrogels. Biomaterials 2006.**27**(19): 3560-3569.

Rajnicek, A., S. Britland, et al. Contact guidance of CNS neurites on grooved quartz: influence of groove dimensions, neuronal age and cell type. Journal of Cell Science 1997.**110**(23): 2905-2913.

Rajnicek, A. and C. McCaig Guidance of CNS growth cones by substratum grooves and ridges: effects of inhibitors of the cytoskeleton, calcium channels and signal transduction pathways. Journal of Cell Science 1997.**110**(23): 2915-2924.

Reis, C. P., R. J. Neufeld, et al. Review and current status of emulsion/dispersion technology using an internal gelation process for the design of alginate particles. Journal of Microencapsulation 2006.**23**(3): 245-257.

Ríhová, B. Immunocompatibility and biocompatibility of cell delivery systems. Advanced Drug Delivery Reviews 2000.**42**(1-2): 65-80.

Ropper, A. H., R. D. Adams, et al. Adams and Victor's principles of neurologyNew York, McGraw-Hill Medical.2009: x, 1572 p.

Sambrook, J. and D. W. Russell Molecular cloning : a laboratory manualCold Spring Harbor, N.Y., Cold Spring Harbor Laboratory Press.2001: 1 v. (various pagings).

Sambrook, J. and D. W. Russell Molecular cloning : a laboratory manualCold Spring Harbor, N.Y., Cold Spring Harbor Laboratory Press.2001: 1 v. (various pagings).

Schmidt, C. and J. Leach Neural tissue engineering: strategies for repair and regeneration. Annu Rev Biomed Eng 2003.**5**: 293 - 347.

Schmidt, C. E. and J. B. Leach NEURAL TISSUE ENGINEERING: Strategies for Repair and Regeneration. Annual Review of Biomedical Engineering 2003.**5**(1): 293-347.

Schubert, D., S. Heinemann, et al. Cholinergic metabolism and synapse formation by a rat nerve cell line. Proc Natl Acad Sci U S A 1977.**74**(6): 2579-2583.

Shaikh, F. M., A. Callanan, et al. Fibrin: a natural biodegradable scaffold in vascular tissue engineering. Cells Tissues Organs 2008.**188**(4): 333-346.

Shibata, A., M. V. Wright, et al. Unique responses of differentiating neuronal growth cones to inhibitory cues presented by oligodendrocytes. Journal of Cell Biology 1998.**142**(1): 191-202.

Shoichet, M. S. Polymer Scaffolds for Biomaterials Applications. Macromolecules 2009.**43**(2): 581-591.

Sofroniew, M. V., C. L. Howe, et al. Nerve growth factor signaling, neuroprotection, and neural repair. Annu Rev Neurosci 2001.**24**: 1217-1281.

Soon-Shiong, P., M. Otterlie, et al. An immunologic basis for the fibrotic reaction to implanted microcapsules. Transplant Proc 1991.**23**(1 Pt 1): 758-759.

Sorribas, H., C. Padeste, et al. Photolithographic generation of protein micropatterns for neuron culture applications. Biomaterials 2002.**23**(3): 893-900.

Stirling, R. V. and S. A. Dunlop The dance of the growth cones--where to next? Trends Neurosci 1995.**18**(2): 111-115.

Stokols, S. and M. H. Tuszynski Freeze-dried agarose scaffolds with uniaxial channels stimulate and guide linear axonal growth following spinal cord injury. Biomaterials 2006.**27**(3): 443-451.

Straley, K. S., C. W. Foo, et al. Biomaterial design strategies for the treatment of spinal cord injuries. J Neurotrauma 2010.**27**(1): 1-19.

Stubbe, B. G., F. Horkay, et al. Tailoring the swelling pressure of degrading dextran hydroxyethyl methacrylate hydrogels. Biomacromolecules 2003.**4**(3): 691-695.

Subramanian, A., U. Krishnan, et al. Development of biomaterial scaffold for nerve tissue engineering: Biomaterial mediated neural regeneration. Journal of Biomedical Science 2009.**16**(1): 108.

Taguchi, T., M. Shiraogawa, et al. A study on hydroxyapatite formation on/in the hydroxyl groups-bearing nonionic hydrogels. J Biomater Sci Polym Ed 1999.**10**(1): 19-32.

Tai, H.-C. and H. M. Buettner Neurite Outgrowth and Growth Cone Morphology on Micropatterned Surfaces. Biotechnology Progress 1998.**14**(3): 364-370.

Tanaka, E. and J. Sabry Making the connection: cytoskeletal rearrangements during growth cone guidance. Cell 1995.**83**(2): 171-176.

Tessier-Lavigne, M. and C. S. Goodman The Molecular Biology of Axon Guidance. Science 1996.**274**(5290): 1123-1133.

Thiele, H. Richtwirkung von Ionen auf anisotrope Kolloide-Ionotropie. Naturwissenschaften 1947.**34**(4): 123-123.

Thumbs, J. and H. H. Kohler Capillaries in alginate gel as an example of dissipative structure formation. Chemical Physics 1996.**208**(1): 9-24.

Tsuruma, A., M. Tanaka, et al. Topographical control of neurite extension on stripe-patterned polymer films. Colloids and Surfaces A: Physicochemical and Engineering Aspects 2006.**284-285**: 470-474.

Verreck, G., I. Chun, et al. Preparation and physicochemical characterization of biodegradable nerve guides containing the nerve growth agent sabeluzole. Biomaterials 2005.**26**: 1307 - 1315.

Wang, A., Q. Ao, et al. Porous chitosan tubular scaffolds with knitted outer wall and controllable inner structure for nerve tissue engineering. J Biomed Mater Res A 2006.**79**(1): 36-46.

Willenberg, B. J., T. Hamazaki, et al. Self-assembled copper-capillary alginate gel scaffolds with oligochitosan support embryonic stem cell growth. Journal of Biomedical Materials Research Part A 2006.**79A**(2): 440-450.

Yang, Y., M. Liu, et al. Effect of chitooligosaccharide on neuronal differentiation of PC-12 cells. Cell Biology International 2009.**33**(3): 352-356.

Yu, T. T. and M. S. Shoichet Guided cell adhesion and outgrowth in peptide-modified channels for neural tissue engineering. Biomaterials 2005.**26**(13): 1507-1514.

Zheng, Y., X. Huang, et al. Performance and characterization of irradiated poly(vinyl alcohol)/polyvinylpyrrolidone composite hydrogels used as cartilages replacement. Journal of Applied Polymer Science 2009.**113**(2): 736-741.

Zhenhuan Zheng, Yujun Wei, et al. Surface Properties of Chitosan Films Modified with Polycations and Their Effects on the Behavior of PC12 Cells. Journal of Bioactive and Compatible Polymers 2009.**24**(1): 63-82.

Zhou, T., B. Xu, et al. Neurons derived from PC12 cells have the potential to develop synapses with primary neurons from rat cortex. Acta Neurobiol Exp (Wars) 2006.**66**(2): 105-112.

Annexure

ANNEXURE

Reagents and Buffers

DMEM F12 1:1 Complete Media

For 50 mL

DMEM : F12 1:1 solution	42.2 mL
Fetal Bovine serum	5 mL
Fetal Horse serum	2.5 mL
Penicillin solution	50µL
Streptomycin solution	50µL

DMEM : F12 1:1 mixture is made by dissolving 15.7 g in 1 L of sterile distilled water. Penicillin stock solution (1 lakh U/mL) is made by dissolving 30.165 mg of Penicillin in 500 µL of sterile distilled water. Streptomycin stock solution (1 µg/mL) is made by dissolving 100 mg of streptomycin in 1 mL of sterile distilled water. Stored at 4°C.

DMEM F12 1:1 PC 12 Differentiation Media

For 50 mL

DMEM : F12 1:1 solution	49.4 mL
Fetal Bovine serum	500 µL
Penicillin solution	50µL
Streptomycin solution	750µL

DMEM : F12 1:1 mixture is made by dissolving 15.7 g in 1 L of sterile distilled water. Penicillin stock solution (1 lakh U/mL) is made by dissolving 30.165 mg of Penicillin in 500 µL of sterile distilled water. Streptomycin stock solution (1 µg/mL) is made by dissolving 100 mg of streptomycin in 1 mL of sterile distilled water. Stored at 4°C.

Nerve Growth Factor – 7S stock solution

Nerve growth factor – 7S	1 mg
Sterile distilled water	1 mL

Stored at -20°C

Phosphate Buffered Saline

NaCl	140 mM
Phosphate buffer	15 mM

To prepare 10 X stock solution, dissolve NaCl (82 g), Sodium phosphate monobasic ($NaH_2PO_4.2\ H_2O$) and Sodium phosphate monobasic ($NaH_2PO_42H_2O$, 4.3 g) and Sodium phosphate dibasic (NaH_2PO_4, 17.4 g). Autoclaved, filter sterilized and stored at 4° C.

10 X poly-L-lysine solution

Poly-L-Lysine hydrobromide	10 mg
Sterile distilled water	10 mL

Stored at 4°C. Working solution concentration 1 X

10 X TAE

For 1 litre

Tris base	48.4 g

Glacial acetic acid	10.9 g
EDTA	2.92g

Dissolve in total volume of 1 L sterile distilled water.

10 X TE Buffer

1 M Tris	10 mL
0.5 EDTA	2 mL

Dissolved and made upto 100 mL with sterile distilled water. pH was adjusted to 7.4-7.6. Filter sterilized and autoclaved. Stored at 4°C. Working concentration is 0.1 X.

2.5 M $CaCl_2$

$CaCl_2$.2 H2O	18.375 g

Dissolve and made upto 50 mL with sterile distilled water. Autoclaved and filter sterilized.

2X HEPES Buffered Saline

140 mM	NaCl
1.5 mM	Na_2HPO_4. 2 H2O
50 mM	HEPES

Dissolve 0.8 g of NaCl, 0,027 g of Na2 HPO4.2 H20 and 1.2 g f HEPES in a total of 90 mL sterile distilled water. pH was adjusted to 7.05 with 0.5 N NaOH. And the final volume was adjusted to 100 mL with distilled water. Filter sterilize and store as 5 mL aliquots at -20°C.

1% Alginate sol

Sodium Alginate	1g
Sterile distilled water	100 mL

1 g of sodium alginate was dissolved in 100 mL sterile distilled water. Mixed thoroughly. Stored at 4° C.

2% Alginate sol

Sodium Alginate	2g
Sterile distilled water	100 mL

2 g of sodium alginate was dissolved in 100 mL sterile distilled water. Mixed thoroughly. Stored at 4° C.

1 M Copper Nitrate

$Cu(NO_3)_2 . 3 H_2O$	24.16g

24.16 g of copper nitrate was dissolved in 100 mL sterile distilled water. Stored at room temperature.